

## Where is the future of pyroelectric infrared detectors in infrared imaging?

Hu Xin-Feng<sup>1,2#</sup>, Wu Bin-Min<sup>1#</sup>, Wang Xu-Dong<sup>1,2,6\*</sup>, Meng Xiang-Jian<sup>1,2,3,6\*</sup>, Wang Jian-Lu<sup>1,4,5\*</sup>, Chu Jun-Hao<sup>1,2,4\*</sup>

1. State Key Laboratory of Infrared Physics, Shanghai Institute of Technical Physics, Chinese Academy of Sciences, No. 500 Yutian Road, Shanghai 200083, China;
2. University of Chinese Academy of Sciences, No. 19 A Yuquan Road, Beijing 100049, China;
3. Yiwu Research Institute, Fudan University, Yiwu, Zhejiang 322000, China;
4. Institute of Optoelectronics, College of Future Information Technology, Fudan University, Shanghai 200433, China;
5. State Key Laboratory of Integrated Chips and Systems, College of Integrated Circuits and Micro-Nano Electronics, Frontier Institute of Chip and System, Fudan University, Shanghai 200433, China;
6. Shanghai Key Laboratory of Optical Coatings and Spectral Modulation, No. 500 Yutian Road, Shanghai 200083, China)

**Abstract:** Pyroelectric detectors, a typical type of uncooled infrared detectors, are widely used in fields such as flame and fire warning, moving target sensing, gas detection, temperature measurement, and even terahertz detection, owing to their high sensitivity, fast response speed, low power consumption, and broad spectral response. Beyond conventional applications, pyroelectric detectors offer irreplaceable advantages in several specialized scenarios, including laser parameter measurement, high-precision spectrometers, spectral response calibration for infrared detectors, as well as applications in space science such as infrared earth sensors and Earth radiation budget measurement. However, in the compelling field of infrared imaging, pyroelectric detectors indeed lose the competition against bolometers, which are another important type of uncooled infrared detector. The review summarizes the intrinsic technical challenges faced by traditional pyroelectric detectors in imaging applications, including difficulties in integration with readout circuits, the requirement for a chopper, and the limitations in miniaturizing pixel size. This article summarizes two technical solutions that can address the difficulties of traditional pyroelectric detectors in infrared imaging: the thermal reset mode and the active detection mode. Through technological development and iteration, pyroelectric focal plane array devices are expected to achieve higher sensitivity and lower cost, securing a place in the application field of infrared imaging technology.

**Key words:** pyroelectric detectors, uncooled infrared imaging, bolometers, focal plane arrays, thermal reset mode

## Introduction

With the advancement of technology, uncooled technology is gradually maturing, leading to a significant drop in the cost of infrared radiation detection and increasingly lower requirements for the environment, equipment, and operator skills. It is no longer a specialized tool exclusive to cutting-edge fields such as military, aerospace, and scientific research<sup>[1-4]</sup>, but is evolving into an infrastructure ubiquitous in modern life<sup>[5-9]</sup>. Infrared detection can capture information beyond sight and touch, such as subtle heat patterns, energy exchanges, and early warning signs of equipment failure. Any object with a temperature above absolute zero emits infra-

red radiation, and the radiation intensity varies with temperature. Based on this principle, infrared detection can help identify locations of heat loss in concrete structures in the construction sector, thereby optimizing designs that are difficult to assess with the naked eye<sup>[10, 11]</sup>. In firefighting, it can penetrate dense smoke to quickly locate trapped victims and fire sources<sup>[12, 13]</sup>. In industrial production, overheating of equipment often precedes a failure; infrared sensors can monitor critical equipment around the clock, ensuring continuous operation of production lines<sup>[14, 15]</sup>. Furthermore, autonomous driving also leverages infrared detection to pierce through rain and darkness, providing a critical technical safeguard for the

**Foundation items:** This work is supported by the National Natural Science Foundation of China (Grant Nos. 62588101, 62535018, 62404232), Department of Science and Technology of Yunnan Province (Grant No. 202402AC080002), China National Postdoctoral Program for Innovative Talents (Grant No. BX20240394), China Postdoctoral Science Foundation (Grant No. 2024M763410), Shanghai Post-doctoral Excellence Program (Grant No. 2024797).

\* **Corresponding author:** e-mail: wxd0130@mail. sitp. ac. cn; xjmeng@mail. sitp. ac. cn; jianluwang@fudan. edu. cn; jhchu@mail. sitp. ac. cn

perception system<sup>[16-18]</sup>.

At the technological core of the above changes lies the infrared radiation detection device, namely infrared detectors. The two principal types of infrared detectors are photon detectors and thermal detectors<sup>[19-21]</sup>. In photon detectors, the absorbed photons directly produce free electrons or holes. In thermal detectors, the absorbed photons produce a temperature change, which is then indirectly detected by measuring a temperature-dependent property of the detector material<sup>[19, 20]</sup>. From an objective perspective, the application and widespread adoption of infrared sensing technology are largely driven by uncooled infrared detectors. Compared to cooled infrared detectors, uncooled infrared detectors offer several advantages: (1) Small size and light weight: They eliminate the need for cryogenic cooling systems, making them easy to integrate into portable devices; (2) Low cost: The core materials and processes are relatively simple, significantly reducing manufacturing costs; (3) Low power consumption and fast startup: They can operate immediately upon power-up, without waiting for a cooler to cool down; (4) Long lifespan and high reliability: With no moving parts like a cooler, the system is more stable and durable. However, their disadvantages include relatively lower sensitivity and slower response speed, and their performance in detecting subtle temperature differences and high-speed moving targets is inferior to that of high-performance cooled detectors. Nevertheless, their performance is already sufficient to meet the requirements of many civilian applications and some military needs<sup>[22, 23]</sup>.

Uncooled infrared detectors can be subdivided into several types, including pyroelectric detectors, bolome-

ters, thermopiles, Micro-Electro-Mechanical Systems (MEMS), Golay cells, etc<sup>[24]</sup>. Among them, the most widely applied are pyroelectric and bolometer detectors. The performance of pyroelectric detectors and bolometers is widely debated, with differing views on which outperforms the other. Detector performance includes parameters such as responsivity, response speed, spectral response range, dynamic range and more. Since pyroelectric detectors and bolometers operate on different principles and are intended for different application scenarios, it is difficult to make a direct comparison between the two using only a few parameters. Pyroelectric detectors operate on the pyroelectric effect, responding solely to the rate of temperature change, and thus exhibit alternating current (AC) response<sup>[25-27]</sup>. Bolometers, in contrast, operate on the temperature coefficient of resistance and exhibit direct current (DC) response<sup>[21, 24]</sup>. The distinction in their operating principles inherently determines that each demonstrates its respective advantages in different application scenarios. Currently, infrared imaging technology is witnessing increasingly extensive applications and has attracted the greatest attention<sup>[28]</sup>. In this domain, pyroelectric detectors indeed fall behind bolometers. Although a lot of previous studies have provided summaries of pyroelectric detectors and their applications, only a limited few have conducted comparative analyses between pyroelectric detectors and bolometers. Furthermore, reports elucidating the reasons why pyroelectric detectors fall behind bolometers specifically in infrared imaging technology are quite rare. Nevertheless, in numerous specialized fields, pyroelectric detectors continue to serve applications for which they are difficult to substitute, as shown in Fig. 1<sup>[25, 28]</sup>.

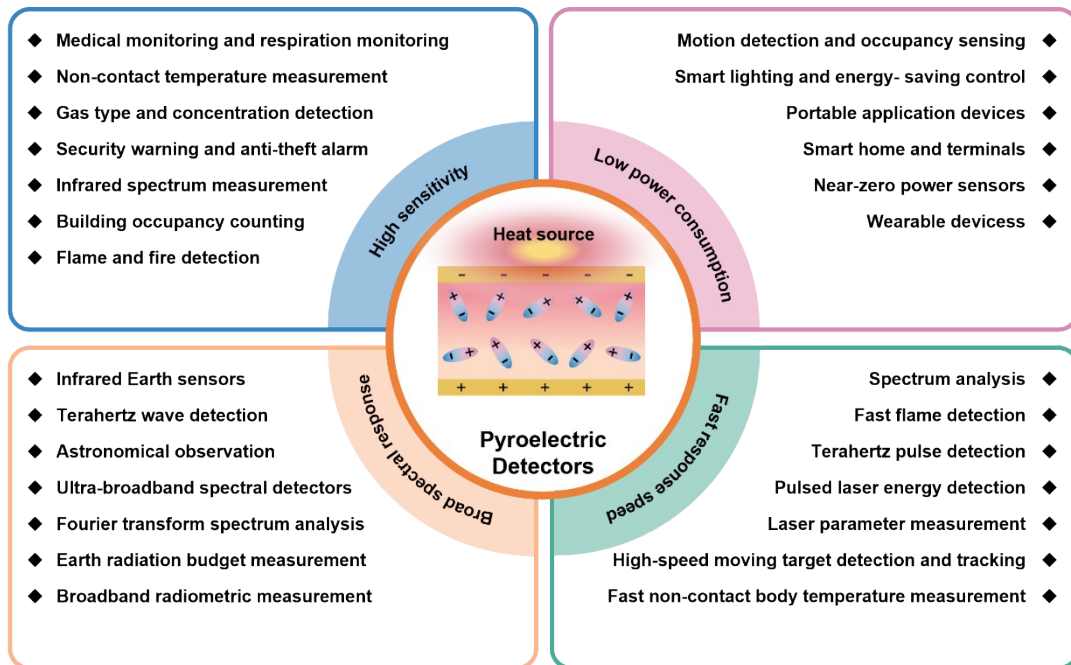


Fig. 1 Pyroelectric detectors feature high-sensitivity, high-speed, low-noise, an ultra-wide flat spectral response, and high-robustness, and are therefore used in numerous fields.

图1 热释电探测器具有高灵敏度、高速、低噪声、超宽平坦光谱响应和高鲁棒性等特点,因此在众多领域得到广泛应用。

In this review, firstly we present the operating principle of pyroelectric detectors and their significant applications across different scenarios. Subsequently, we discuss the development of pyroelectric detectors and bolometers in uncooled infrared imaging technology, as well as the reasons for the relative inferiority of pyroelectric detectors compared to bolometers. Following that, we propose technical approaches to overcome the constraints by limiting pyroelectric infrared focal plane array detectors. Finally, we offer a perspective on the potential of pyroelectric detectors in future infrared imaging applications.

## 1 Principles and characteristics of pyroelectric detectors

Given that numerous articles and books provide detailed descriptions of the working principle of pyroelectric detectors, interested readers may refer to the relevant literatures<sup>[29]</sup>. This review focuses on the structure of pyroelectric detectors and several key performance parameters, including responsivity, noise equivalent power, and specific detectivity. The working principle of the pyroelectric detector is based on the pyroelectric effect, which is present in all polar materials that exhibit a change in electric polarization  $\Delta p$  when a temperature variation  $\Delta T$  is applied uniformly. The polarization change caused by temperature variation  $\Delta T$  can be expressed as:

$$P = p\Delta T \quad (1)$$

where  $p$  is the pyroelectric coefficient. The generated pyroelectric charge  $Q$  is:

$$Q = pA\Delta T \quad (2)$$

where  $A$  is the detector area. The corresponding current  $I_{ph}$  is:

$$I_{ph} = Ap \frac{dT}{dt} \quad (3)$$

The current responsivity  $R_i$  is:

$$R_i = \frac{I_{ph}}{\Phi_0} \quad (4)$$

where  $\Phi_0$  is the amplitude of the sinusoidal radiation. This implies an AC-coupled operating mode, where the response is proportional to the rate of temperature change: the faster the temperature changes, the greater the response<sup>[29]</sup>.

A traditional complete pyroelectric detector consists of a sensing element and a signal amplification circuit. The sensing element includes both an electrical structure (Fig. 2 (a)) and a thermal structure (Fig. 2 (b)), while the signal amplification circuit can be further divided into two types: voltage readout and circuit readout configurations (see Fig. 2 (c) and Fig. 2 (d)). The performance of the detector is determined by two parameters: responsivity and noise level. The principle for optimizing device performance is always to maximize responsivity while minimizing noise. By solving the heat balance equation:

$$C_{th} \frac{d\Delta T}{dt} + G_{th} \Delta T = \varepsilon_{th} \Phi \quad (5)$$

where  $C_{th}$  is the heat capacity,  $G_{th}$  is the thermal conductance, and  $\varepsilon_{th}$  is the emissivity of the detector. The temperature change of the thermal detector caused by the incident radiant flux can be obtained as:

$$\Delta T = \frac{\varepsilon_{th} \Phi_0}{(G_{th}^2 |\omega^2 C_{th}^2|)^{1/2}} \quad (6)$$

Combining with Equation (3), the photocurrent is:

$$I_{ph} = \frac{\varepsilon_{th} p A \Phi_0 \omega}{G_{th} (1 \omega^2 \tau_{th}^2)^{1/2}} \quad (7)$$

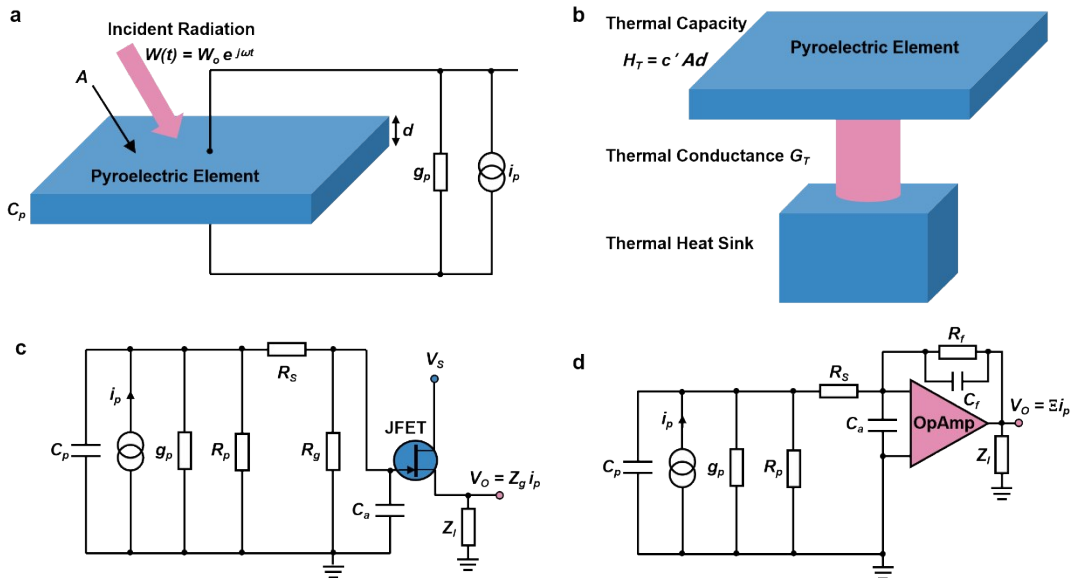


Fig. 2 Thermal and electrical structures of a simple pyroelectric infrared detector: (a) the electrical structure<sup>[29]</sup> and (b) the thermal structure<sup>[29]</sup> of pyroelectric device; The device configurations using (c) a voltage amplifier<sup>[29]</sup> and (d) a current amplifier<sup>[29]</sup>.

图2 简单热释电红外探测器的热结构和电结构:(a)热释电器件的电结构[29];(b)热释电器件的热结构[29];使用(c)电压放大器[29]和(d)电流放大器[29]的器件结构。

The parameters affecting the responsivity of the detector include the pyroelectric coefficient, dielectric constant, and thermal properties of the pyroelectric material, while the overall noise level of the detector is mainly determined by the dielectric loss of the pyroelectric material and the noise of the amplification circuit. Regarding how to select appropriate materials and detector structures, Whatmore and Ward provided a detailed discussion in an article<sup>[29]</sup>.

It is precisely the AC operating mode of the pyroelectric detector that endows it with superior performance in terms of response sensitivity, response speed, and bandwidth<sup>[26, 27, 30-32]</sup>, thereby giving it an irreplaceable role in some important application areas, such as security and surveillance<sup>[33-36]</sup>, flame and fire alarms<sup>[37-40]</sup>, gas monitoring<sup>[41-45]</sup>. Particularly, pyroelectric detectors are broadly reported due to their low power requirement, low manufacturing, fast response and relatively high sensitivity over a wide range of temperature and wide spectral bandwidth. Nowadays, following a fast progress in terahertz (THz) and millimeter-wave (MMW) technologies, working on the improvement of the sensitivity of pyroelectric detection at longer wavelengths far beyond the infrared (IR) range<sup>[29, 30, 46]</sup>. There are also other advantages to pyroelectric detectors that may not be so obvious. For example, pyroelectric detectors are far more robust than other detectors in the presence of thermally high-dynamic scenes. Being AC coupled and therefore lacking offsets, rapid changes in ambient and scene temperatures produce little disturbance to operation. Calibration is far simpler for pyroelectric detector arrays than for microbolometer arrays.

## 2 Application scenarios of pyroelectric detectors

### 2.1 Precision instrument

#### 2.1.1 Laser parameter measurement

Pyroelectric detectors have fast response times and can measure the energy of pulsed lasers as well as the power of continuous-wave (CW) lasers<sup>[47, 48]</sup>, with spectral ranges from 13 to 355 nm and 1.06 to >3000  $\mu\text{m}$ . In laser processing, calibration of medical laser equipment, and scientific research experiments, they are used for real-time monitoring of laser output stability, measuring the energy of individual laser pulses, and mapping the power distribution of laser beams. Note that Ophir Optonics is one of the few companies capable of producing pyroelectric cameras for laser beam mapping analysis, and the core component of the camera is a  $\text{LiTaO}_3$  (LT) focal plane array device. Fig. 3 (a) shows a schematic diagram of a pyroelectric detector measuring pulsed laser energy<sup>[47]</sup>. To evaluate its linearity, two methods are adopted. One is comparative measurement with a calorimeter, and the other uses the physical law that irradiance is inversely proportional to the square of the distance. Fig. 3 (b) shows the linearity measurement by comparison to a LT detector<sup>[47]</sup>. Within the given pulse energy range, the nonlinear deviation of the detector remains at an acceptable level, providing a reference for the error range

in measuring pulsed laser energy.

#### 2.1.2 Terahertz detection

Pyroelectric materials are also sensitive to terahertz radiation (via a thermal absorption mechanism)<sup>[30, 46, 49-51]</sup>, converting extremely low-energy terahertz photons into heat and subsequently into electrical signals. Pyroelectric detectors fabricated from LT can detect frequencies from 0.1 to 30 THz, with noise equivalent power on the order of  $\text{nW}$ <sup>[51-53]</sup>. Fig. 3 (c) shows a schematic diagram of a lithium tantalate pyroelectric detector for THz measurement<sup>[46]</sup>. The detector exhibits good linear response within a low pulse energy range. However, when the pulse energy and fluence exceed a certain threshold, the response shows sublinear saturation, which originates from the transient effect of the strong terahertz electric field on the sensitive element of the detector (Fig. 3 (d))<sup>[46]</sup>. It is evident that in the precise measurement of terahertz radiation, attention must be paid to the linear response characteristics of the detector and calibration must be performed.

#### 2.1.3 Precision temperature measurement

Although less common in steady-state precision compared to thermopiles, pyroelectric detectors combined with choppers (since pyroelectric sensors only respond to changes, continuous radiation must be modulated into alternating signals) can form highly sensitive radiation thermometers. Recently a new design for thermal-infrared radiation thermometer and sensors has been reported by National Institute of Standards and Technology (NIST). Fig. 3 (e) presents a schematic diagram of the Ambient Radiation Thermometer (ART)<sup>[54]</sup>. Critical optical elements, such as the field stop, Lyot stop, collimating lens, and detector (pyroelectric detector), are placed inside a thermally stabilized assembly that is controlled using thermo-electric coolers and thermistors. The assembled radiation thermometer is calibrated using both variable temperature fluid-bath and heat-pipe blackbodies from  $-45^\circ\text{C}$  to  $75^\circ\text{C}$  and the use of a modified-Planck function and these blackbodies. The size-of-source effect both with and without the Lyot stop has been measured. This new design, during operations without the need for cryogenic cooling, demonstrates sub millikelvin temperature measurement resolution with few millikelvin, week-long stable operations while measuring room-temperature objects (Fig. 3 (f))<sup>[54]</sup>. This new design can be immediately used to improve standards-quality radiation thermometers used to validate non-contact temperature scales at calibration laboratories.

#### 2.1.4 Infrared spectral irradiance and radiance responsivity calibrations

Absolute measurement of spectral responsivity for radiance and irradiance in the infrared spectral region has long been an international major challenge, as it has been unable to achieve the low uncertainties attainable in the visible spectral region. Recently, both the NIST in the United States and the Physikalisch-Technische Bundesanstalt (PTB) in Germany have made significant progresses in reducing the measurement uncertainties of infrared spectral responsivity calibrations<sup>[55-58]</sup>. NIST has

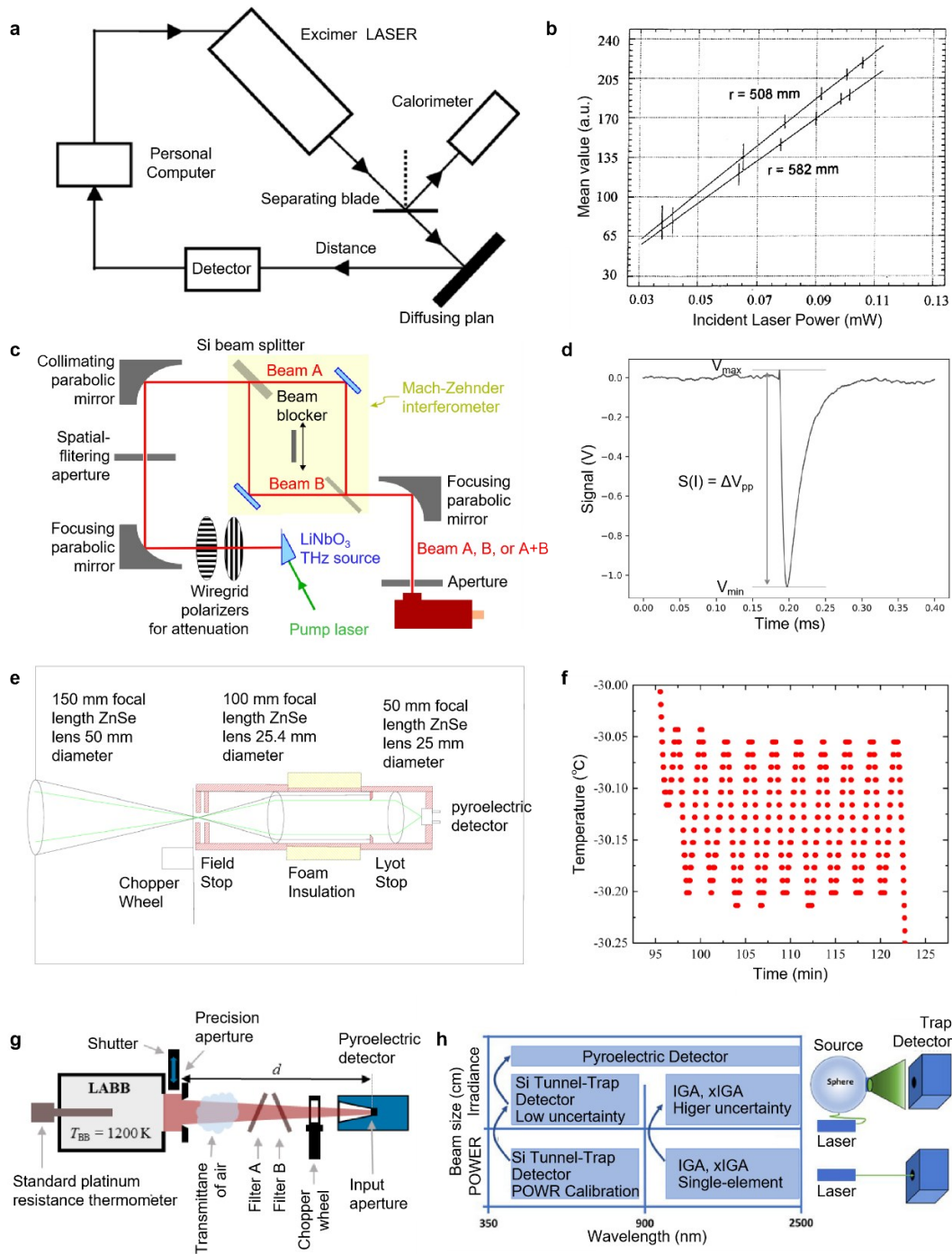


Fig. 3 Pyroelectric detectors applied to precision measurements: (a) Experimental setup for measuring the average energy of a laser<sup>[47]</sup>; (b) Linearity measurement by comparison to a LiTaO<sub>3</sub> detector<sup>[47]</sup>; (c) Schematic diagram of the experimental setup for THz detection<sup>[46]</sup>; (d) Typical voltage response of the detector to a single-cycle THz pulse.  $V_{\min}$  and  $V_{\max}$  are the voltage minimum and maximum, and  $S(I) = \Delta V_{pp}$  is the signal measured for the irradiation flux  $I$ <sup>[46]</sup>; (e) Optical design layout of the ART<sup>[54]</sup>; (f) ART measurements of the ammonia heat-pipe blackbodies (AHPBB) set at  $-30^{\circ}\text{C}$ . The oscillations originate from the control loop algorithm that could not fully stabilize the AHPBB temperatures<sup>[54]</sup>; (g) The figure shows the light source size as a function of wavelength. On the right is a schematic diagram of the illumination geometry<sup>[55]</sup>; (h) Schematic diagram of the test setup for detector calibration. This setup includes a large-area blackbody (LABB) with two transmission filters, and the spectral responsivity is involved in the calibration process<sup>[56]</sup>.

图3 热释电探测器在精密测量中的应用:(a)用于测量激光平均能量的实验装置[47];(b)与钽酸锂探测器比较进行的线性度测量[47];(c)太赫兹探测实验装置示意图[46];(d)探测器对单周期太赫兹脉冲的典型电压响应。 $V_{\min}$ 和 $V_{\max}$ 分别为电压最小值和最大值, $S(I) = \Delta V_{pp}$ 为在辐照通量下测得的信号[46];(e)环境辐射温度计的光学设计布局[54];(f)环境辐射温度计对设定在 $-30^{\circ}\text{C}$ 的氨热管黑体的测量结果。振荡源于控制回路算法未能完全稳定氨热管黑体的温度[54];(g)光源尺寸随波长变化的图示。右侧为照明几何结构的示意图[55];(h)探测器校准测试装置示意图。该装置包括一个大面积黑体和两个透射滤波器,校准过程中涉及光谱响应度[56]。

reduced the measurement uncertainty of short-wave infrared spectral responsivity to below 0.3% using pyroelectric detectors, approaching the measurement uncertainty level of visible spectral region calibrations (Fig. 3 (g))<sup>[56]</sup>. PTB has measured the spectral irradiance responsivity of pyroelectric detectors over a broad infrared wavelength range (from 1.5  $\mu\text{m}$  to 14  $\mu\text{m}$ ) with measurement uncertainties between 1% and 14% (Fig. 3 (h))<sup>[55]</sup>. These studies demonstrate that pyroelectric detectors can serve as transfer standards for the spectral responsivity calibration of other infrared detectors. By further improving detector performance and calibration techniques, the measurement uncertainties can be further reduced, with the potential to reach the calibration levels achieved in the visible spectral range.

## 2.2 Safety monitoring

### 2.2.1 Security and surveillance

A passive infrared (PIR) system detects motion by sensing the infrared radiation emitted by moving objects<sup>[59]</sup>. When an object with a temperature above absolute zero moves across the sensor's field of view, the sensitive pyroelectric material in the sensor undergoes charge separation induced by the temperature change, thereby outputting a weak electrical signal<sup>[36, 60]</sup>. Fig. 4 (a) shows a schematic diagram of the detector identifying human target movement in three different scenarios<sup>[8]</sup>. A photograph of the PIR is shown in Fig. 4 (b), where the sensing area is divided into 14 segments, each corresponding to a binary value<sup>[8]</sup>. When a human target moves within the detection area, the segment that receives the signal outputs 1, while the segment that does not receive the signal outputs 0. Through algorithmic processing (Fig. 4 (c)), the moving human target can be accurately identified. Fig. 4 (d) presents a comparison of the output results after different arithmetic processing<sup>[8]</sup>. To improve detection sensitivity and coverage, a Fresnel lens is usually mounted in front of the pyroelectric sensor in a PIR system. This lens concentrates infrared radiation energy from a wide spatial area onto the tiny sensitive surface of the sensor, significantly extending the detection range and converting motion patterns from different zones into differential signals<sup>[61]</sup>.

Owing to its passive detection, extremely low power consumption, and low cost, PIR sensors have been widely used in intrusion alarm systems, automatic lighting control, access management, and building energy management<sup>[34, 59]</sup>. Fig. 4 (e) shows a schematic diagram of the PIR detecting and identifying a moving human target. The signals when no human target is detected and when a human target is detected are shown in Fig. 4 (f)<sup>[8]</sup>. By optimizing lens design, considering the temperature difference between the environment and the target, and adjusting the partitioning of the sensing area, the effective detection range of an infrared detection system can be extended to 40 meters or even further<sup>[35]</sup>.

In the field of long-range security surveillance, Eltec Instruments has developed an infrared telescope product based on pyroelectric detectors. Its "IR-EYE" series long-range passive infrared thermal imaging tele-

scope for security applications can monitor ranges of approximately 500 feet. It has been widely deployed by various branches of the U. S. military and multiple government agencies for perimeter security, border surveillance, and critical asset protection, and has demonstrated long-term reliability through years of field applications.

### 2.2.2 Smart home and building automation

Utilizes its ability to detect the presence or movement of the human body to act as a trigger switch for automation systems. Automatic lighting: lights automatically turn on when a person enters a hallway or restroom and turn off after a delay when the person leaves<sup>[62]</sup>. Smart appliances: when a room is detected to be unoccupied, the air conditioner temperature is automatically adjusted, or unnecessary appliances are turned off to save energy. Smart bathroom mirrors/toilets: ambient lights or function panels automatically activate upon sensing human proximity. Smart homes and building automation align with the concepts of energy conservation, environmental protection, and green development, offering broad application prospects for pyroelectric detectors<sup>[9, 63]</sup>.

### 2.2.3 Public places and pedestrian flow management

A pyroelectric infrared sensor is a passive infrared detector capable of detecting changes in infrared radiation emitted by the human body, thereby enabling the perception of moving persons<sup>[64]</sup>. When a pedestrian passes through the sensor's field of view, the thermal radiation signal is received by the sensor and converted into an electrical signal for subsequent circuit analysis and counting<sup>[65]</sup>.

Bidirectional counting is a key technology of pyroelectric detectors. It employs two independent sensors installed on the inner and outer sides of a doorway and determines the direction of entry or exit by detecting the sequence in which the pedestrian triggers the sensors. When a person passes from different directions, the two sensing elements receive the infrared radiation in opposite orders, generating alternating signals with opposite phases, thereby accurately discerning the direction of motion<sup>[65]</sup>. More advanced array-type pyroelectric detectors can automatically count bidirectional pedestrian flow by defining virtual counting lines. This technology has been widely applied in personnel counting, direction sensing, and area security. Studies have shown that a personnel counting system based on an eight-element linear array pyroelectric detector achieves an accuracy of over 98% for detecting pedestrians passing through a doorway. In museum visitor monitoring, pyroelectric sensors are used as on-site counting devices<sup>[66, 67]</sup>. Regression analysis indicates a very small discrepancy from manual counting, providing reliable data support for visitor management and exhibit layout optimization<sup>[68, 69]</sup>.

## 2.3 Spectral detection

### 2.3.1 Applications for spectrometers

Pyroelectric detectors are most popular in IR spectroscopy, and they are mainly used in spectrometers in three forms, the first of which is as the core detector of

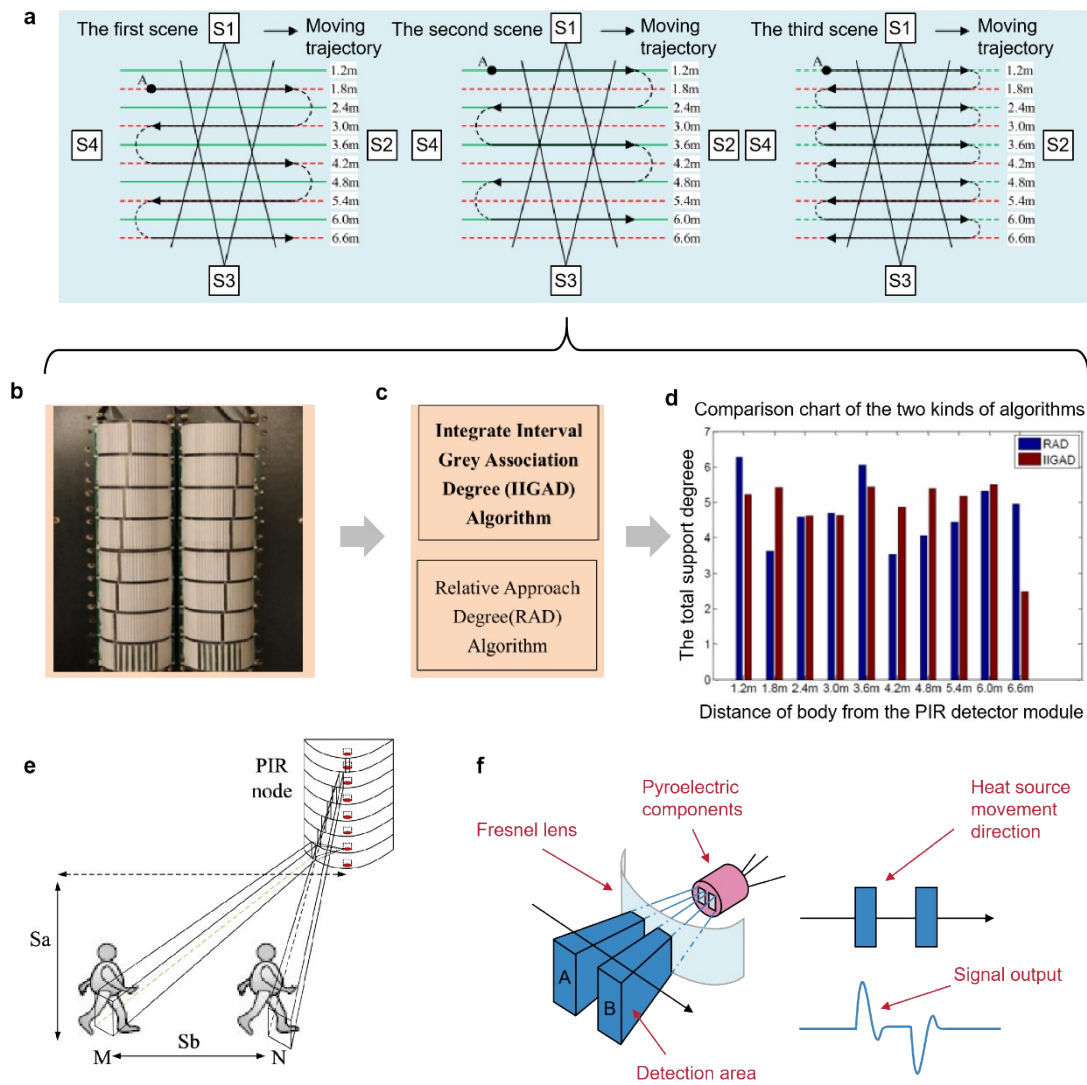


Fig. 4 Pyroelectric detectors applied for safety monitoring: (a) Schematic diagram of identifying the radial distance between a moving object and the detector under different experimental scenarios<sup>[8]</sup>; (b) PIR node<sup>[8]</sup>; (c) Processing of signals obtained from the pyroelectric detector using different algorithms<sup>[8]</sup>; (d) Comparison of the outputs from two algorithms<sup>[8]</sup>; (e) Schematic of detecting human body movement speed<sup>[8]</sup>; (f) Principle of waveform direction<sup>[8]</sup>.

图4 热释电探测器在安全监测中的应用:(a)不同实验场景下确定移动物体与探测器之间径向距离的示意图[8];(b)热释电红外节点[8];(c)使用不同算法处理从热释电探测器获取的信号[8];(d)比较两种算法输出的结果[8];(e)检测人体移动速度的示意图[8];(f)波形方向的原理[8]。

Fourier-transform infrared (FTIR) spectrometers<sup>[70]</sup>. High throughput (greater than 20% of IR beam reaching the IR detector) and static experiments are generally run utilizing a pyroelectric detector, such as deuterated, L-alanine doped triglycine sulfate (DLATGS), because it gives full, specific detectivity ( $D^*$ ) in high-flux environments. From an applications perspective, the DLATGS detector provides linear response over a wide range of FT-IR throughput, which is beneficial in qualitative and quantitative FTIR sampling<sup>[71-73]</sup>. Second, it is used as a reference detector in FTIR spectrometers. To measure semiconductor-based infrared photon detector spectral response, a FTIR is commonly employed with a pyroelectric detector as the reference detector. In this measurement, each wavelength of light is modulated by the FTIR into an interferogram whose frequency content is propor-

tional to the wavenumber of the source radiation which, when combined with the frequency dependent response of the pyroelectric detector, perturbs the reference detector spectral shape. A correction to this perturbation is demonstrated by using the transfer function of the pyroelectric detector and voltage amplifier system. Fig. 5 (a) is a schematic diagram of using a pyroelectric detector to calibrate laser parameters, taking advantage of its ability to operate stably in a high fluence environment. Fig. 5 (b) shows the actual calibration results, indicating that the pyroelectric detector exhibits good linear response to optical signals of different energy densities. The third application is the special use of pyroelectric detectors in portable infrared spectrometers. In 2014, Kim et al reported an ultra-compact attenuated total reflectance spectrophotometer whose frequency band was 5.5-11.0  $\mu\text{m}$

with a linear variable filter, and a pyro-electric array detector<sup>[74]</sup>. When using two-dimensional materials to construct photodetectors, a rational band design can effectively improve the signal-to-noise ratio while significantly reducing the device footprint<sup>[75]</sup>. However, photodetectors fabricated in this manner have a limited detection band, making it difficult to achieve a broad spectral response. Recently a compact infrared attenuated total reflection spectrometer using a pyroelectric detector array has been evaluated and compared to a conventional laboratory FTIR system for applications in food analysis<sup>[76]</sup>. Of particular interest is the fact that the comparison of compact devices with conventional FTIR spectrometers yields similar analytical performance characteristics, which facilitates a multitier analytical concept combining medium-resolution in-field data with high-resolution laboratory data.

### 2.3.2 Industrial and process monitoring

Pyroelectric detectors utilize the characteristic that the spontaneous polarization of pyroelectric materials varies with temperature, converting changes in infrared radiation into electrical signals to achieve highly sensitive non-contact detection of dynamic heat sources. Such detectors can operate at room temperature, achieving high sensitivity without the need for cooling, and exhibit frequency characteristics superior to traditional bolometers, demonstrating unique application value in industrial process monitoring<sup>[42]</sup>.

Pyroelectric detectors can monitor temperature changes in real time during industrial equipment operation, enabling early warning of motor overheating or bearing faults. Their circuit design focuses on extracting the AC component of the signal and performing envelope detection to capture temperature trends rather than absolute values. For overheating phenomena in high-temperature equipment such as furnaces and engine exhaust devices, flame sensors based on lithium tantalate single crystals can timely warning of various fire hazards. Furthermore, pyroelectric sensors can be used to detect products moving along production lines that possess specific thermal characteristics, such as newly manufactured glass bottles and hot metal castings. Infrared thermography can also identify crack defects in products on production lines in a

non-contact manner within seconds.

## 2.4 Space and astronomy applications

### 2.4.1 Earth sensors

The earth sensor is an important payload in the space sector, used for attitude control of space vehicles. The Earth's atmosphere absorbs and emits infrared radiation at specific wavelengths, while space is cold. Pyroelectric detectors (often combined with scanning mechanisms) determine the position of the "horizon" by detecting the abrupt boundary of infrared radiation between the Earth and space. On low-Earth orbit satellites, earth sensors help the satellite determine its orientation relative to Earth, thereby adjusting the angle of solar panels or the direction of antennas. Fig. 6 (a) illustrates the working principle of an earth sensor. During spacecraft operation, the detector continuously scans within a certain angular range. When the detector scans from space to the Earth, the signal output changes from a low level to a high level. Conversely, when the detector scans from the Earth to space, the signal output changes from a high level to a low level. Fig. 6 (b) shows the composition of the earth sensor. The core components are a scanning mirror system, an infrared telescope, an analogue signal processor, and a digital signal processor<sup>[77]</sup>. Fig. 6 (c) presents a schematic diagram of the relative position between the earth sensor and the Earth when the spacecraft is in correct and incorrect attitudes<sup>[78]</sup>. To illustrate the working principle of the earth sensor more vividly, Fig. 6 (d) shows a three-dimensional schematic diagram of its operating principle<sup>[78]</sup>.

Servo Corporation of America is pioneer in Infrared Detectors, Infrared Subsystems for Satellite Attitude Determination and Radio Direction Finding Equipment for airports and harbors. In the 1980s Servo developed a pyroelectric detector made of LT, specifically designed for space flight. Pyroelectric detectors, made of LT, are not only less expensive to build but they are much more sensitive devices than either the traditional bolometers or thermopiles. They have introduced an Earth Sensor with an operational life of 15 years in geostationary earth orbit.

### 2.4.2 Earth radiation budget measurement

The Earth Radiation Budget (ERB) refers to, on

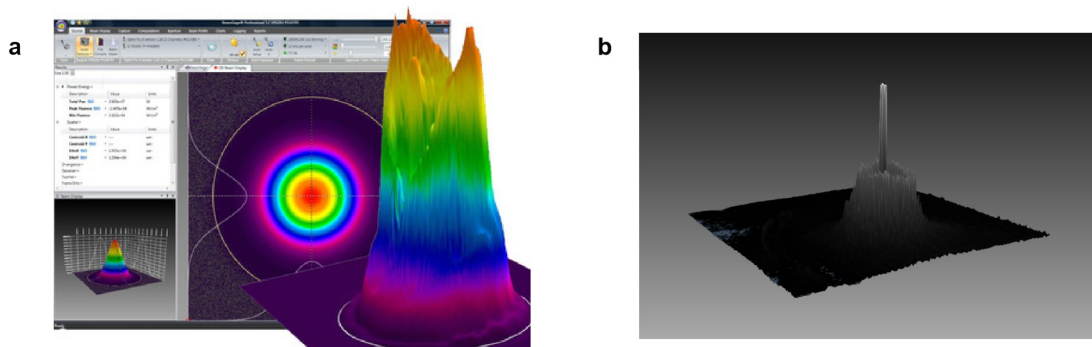


Fig. 5 Pyroelectric detectors applied to spectral detection: (a) Schematic diagram of laser calibration; (b) Laser calibration using a pyroelectric detector.

图5 热释电探测器在光谱检测中的应用:(a)激光校准示意图;(b)使用热释电探测器进行激光校准。

one hand, the incoming shortwave radiation from the Sun (solar radiation), and on the other hand, the outgoing longwave infrared energy radiated by the Earth into outer space. Achieving long-term, continuous, and globally covered ERB monitoring is the core data source for quantifying climate forcing, evaluating model accuracy, and predicting future trends<sup>[79, 80]</sup>. Satellite platforms are the best means to accomplish this task. Major international observation systems (such as NASA's Clouds and the Earth's Radiant Energy System) and the payloads onboard China's Fengyun satellites have already been able to "see" the total balance of this budget from space, typically using broadband bolometers<sup>[81]</sup>. However, to understand how this energy is distributed and evolves, broadband Fourier spectrometers are required. Pyroelectric detectors, due to their high sensitivity and fast response speed, are the best choice for constructing such spec-

trometers. To this end, the European Space Agency (ESA) has specifically planned the Far-infrared Outgoing Radiation Understanding and Monitoring (FORUM) mission, whose core payload is a FORUM Sounding Instrument (FSI) covering the range of 6.25-100  $\mu\text{m}$ , which will perform the first spectral measurement of Earth's longwave radiation from space<sup>[79, 82]</sup>. The core component of FSI is a pyroelectric detector<sup>[83]</sup>. Fig. 6 (e) shows a schematic diagram of the pointing unit of the FSI, which is primarily responsible for controlling the detection direction. The FORUM Embedded Imager (FEI) also uses this pointing unit. In addition, the FSI and FEI share a calibration unit, shown schematically in Fig. 6 (f), which is mainly responsible for measurement accuracy.

### 3 Why do pyroelectric detectors lose to

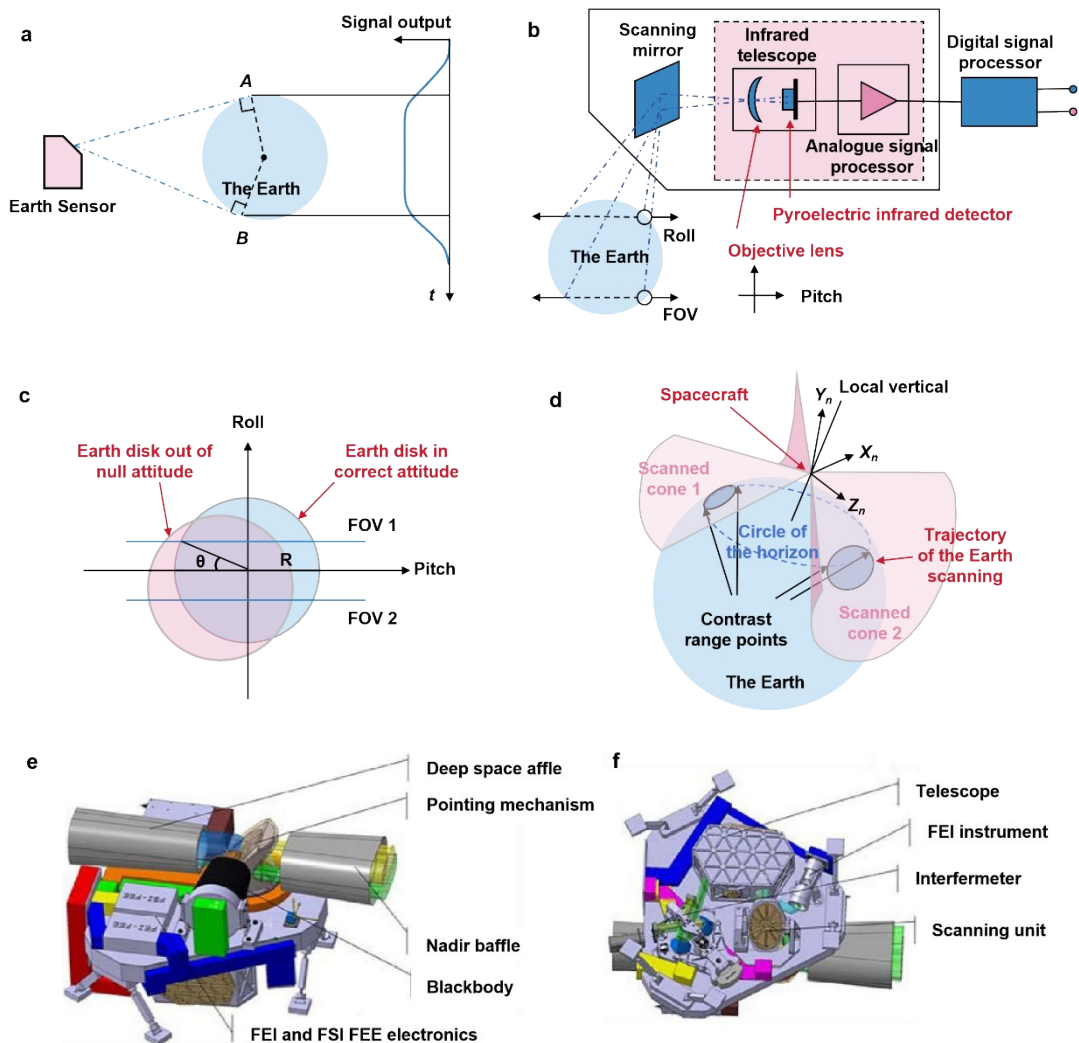


Fig. 6 Pyroelectric detectors applied to space and astronomy: (a) Schematic diagram of the working principle of an earth sensor; (b) Composition of the earth sensor<sup>[77]</sup>; (c) Earth disk as seen from geostationary altitude with the sensor in correct and out of null attitude conditions<sup>[78]</sup>; (d) Secant type scanning principle for the Earth Orientation Device<sup>[78]</sup>; (e) Schematic diagram of the pointing unit, which is responsible for controlling the detection direction; (f) Schematic diagram of the calibration unit, which is responsible for measurement accuracy.

图6 热释电探测器在太空和天文学中的应用:(a)地球传感器的工作原理示意图;(b)地球传感器的组成[77];(c)从地球同步轨道视角看到的地球圆盘,传感器处于正确姿态和错误姿态时的情况[78];(d)地球定向装置的切线扫描原理[78];(e)负责控制探测方向的指向单元的示意图;(f)负责测量精度的校准单元的示意图。

## bolometers in thermal imaging technology?

### 3.1 Uncooled infrared imaging technology

The detectors used for infrared thermal imaging are all focal plane arrays (FPAs) devices<sup>[84, 85]</sup>. The first pyroelectric detector array was produced at Raytheon began in the mid-1970s in what was formerly the Texas Instruments Defense Systems and Electronics Group. The production detector array is based on hybrid technology, which consists of an array of  $\text{Ba}_x\text{Sr}_{1-x}\text{TiO}_3$  (BST) pixels bump-bonded to a readout integrated circuit (ROIC), providing gain and noise filtering for each pixel. The array contains approximately 80,000-pixels in a  $240 \times 320$  format. The technology was demonstrated to the military for the first time in 1979. The noise equivalent temperature difference (NETD) is the commonly used figure-of-merit for infrared-imaging systems using FPAs, and the NETD as low as 40 mK (array average) have been demonstrated with the BST hybrid technology<sup>[86, 87]</sup>.

At the same time however, another technology was developed: microbolometer technology. The basic principle of a bolometer is as follows: a thermistor element made of a material with a high temperature coefficient of resistance [such as vanadium oxide ( $\text{VO}_x$ ) or amorphous silicon (a-Si)] absorbs incident infrared radiation, causing a corresponding change in its resistance. Peripheral circuitry then converts this resistance change into a quantifiable electrical signal for output, thereby enabling detection of the radiation power<sup>[88]</sup>. Currently, the core of this technology lies in its high level of integration with the ROIC, that is, fabricating the detector array directly on the wafer containing the ROIC<sup>[89]</sup>. Furthermore, it is necessary to reduce the noise level of the ROIC and increase its frame rate. The U. S. military provided funding to develop thermal imaging technology into equipment systems including rifle sights and driver vision enhancement systems. They strongly believed in thermal imaging systems with uncooled detectors and wanted to further develop both BST and  $\text{VO}_x$  detector technology<sup>[90]</sup>. However, the mainstream technical route for bolometers relies on microelectromechanical systems

(MEMS) to fabricate microbridge structures on standard semiconductor production lines, thereby achieving thermal isolation. A typical fabrication process involves sequentially depositing a sacrificial layer, a structural layer, a thermistor layer, and electrodes on the readout circuit, and then releasing the sacrificial layer to form a suspended detection structure<sup>[91]</sup>. In contrast, BST adopts a different hybrid process, such as flip chip bonding. Because this process suffers from deficiencies in integration density and thermal isolation capability, it is gradually being replaced by the MEMS process. Around late 1990s, convinced of the advantages  $\text{VO}_x$  has over BST, the US Military decided not to provide any more funding for research into BST technology. From that point in time, only further research in  $\text{VO}_x$  was supported<sup>[92]</sup>, meaning that in the field of infrared thermal imaging technology, bolometers have completely dominated over pyroelectric detectors<sup>[22, 93]</sup>. Today, complementary metal-oxide-semiconductor (CMOS) compatible microbolometer products with excellent performance have become available on the market. Benefiting from mature semiconductor processes, such devices can be mass produced, thereby effectively reducing the manufacturing cost of bolometers<sup>[94, 95]</sup>. In terms of development trends, increasing the density of detector arrays by reducing the pixel pitch is becoming an important technical pathway to further enhance integration and lower costs<sup>[94]</sup>.

### 3.2 The reasons that pyroelectric detectors lost to bolometers

In terms of working principle, pyroelectric detectors have potentially higher sensitivity, faster response speed, and lower power consumption than bolometer detectors<sup>[21, 96, 97]</sup>. Performance comparison between pyroelectric detector and bolometer is shown in Table 1. So why did pyroelectric detectors lose to bolometers in infrared thermal imaging technology? The author considers that pyroelectric imagers lost the competition against bolometers for three major reasons: 1) the need for a chopper, 2) the inability to effectively reduce pixel size, and 3) higher difficulty in integrating with ROIC.

#### 3.2.1 The issues brought by the chopper

Pyroelectric detectors usually employ ferroelectric

Table 1 Performance comparison between pyroelectric detector and bolometer.

表 1 热释电探测器和测辐射热计的性能对比

Detector type	Sensitivity temperature coefficient	NETD	Detectivity	Response time	References
Pyroelectric detector	Pyroelectric coefficient: ( $\mu\text{C m}^{-2} \text{K}^{-1}$ )				
	$\text{LiTaO}_3$ : 180~280	40 mK	$10^6 \text{ cm Hz}^{1/2} \text{W}^{-1}$	10 ms	[32, 51, 98~103]
	$\text{LiNbO}_3$ : 40~90	~200 mK	$\sim 10^8 \text{ cm Hz}^{1/2} \text{W}^{-1}$	~100 ms	
	PVDF: 20~45				
	PZT: 300~800				
TCR:					
Bolometer	$\text{VO}_x$ :	30 mK	$10^7 \text{ cm Hz}^{1/2} \text{W}^{-1}$	1 ms	[92, 104~109]
	-2%/K~-5%/K	~100 mK	$\sim 10^9 \text{ cm Hz}^{1/2} \text{W}^{-1}$	~20 ms	
	a-Si:				
	-2%/K~-3%/K				

materials having an intrinsic internal polarization that is, at least to some degree, aligned normal to the plates of the capacitor. If the temperature of the open-circuit capacitor changes and then remains constant for a prolonged period, the voltage developed will diminish over time as current leaks through the ferroelectric material and compensates for the change in polarization. This is why a chopper is required when a pyroelectric infrared focal plane array performs staring imaging of a target<sup>[110]</sup>.

Indeed, the chopped radiation detection mode offers many advantages, including virtually no thermal drift, excellent dynamic compensation for thermal shock, unequaled noise filtering, high optical resolution, and fast response times<sup>[111]</sup>. However, the use of a chopper also brings some negative effects, including reduced exposure time of the detecting element to the scene, increased difficulty in reducing the size of the detecting element, higher cost, and reduced reliability. As the chopper rotates, the temperature of each pixel fluctuates periodically. Signal is optimized when the time of obscuration is equal to the time of exposure, leaving only 50% of the total available time for collecting signal<sup>[112]</sup>. The electrical signal is generated by clamping the output at one extreme of the thermal wave and reading the signal at the next extreme. There are therefore alternating positive and negative signals. The negative signals are inverted and can then be added to the positive signals for improved responsivity. Although the design of the readout circuit can convert negative signals into positive ones, thereby improving the responsivity, even an ideal circuit design results in a signal loss of at least 30%<sup>[110]</sup>.

### 3.2.2 The difficulty in reducing the size of the pyroelectric detection element

The large pyroelectric current requires that pyroelectric should possess a large surface area, a large pyroelectric coefficient, and a high rate of temperature change. Therefore, the inherent requirement for a large sensitive area in pyroelectric detection conflicts with the demand for small-pixel, large-scale focal plane arrays<sup>[113]</sup>. As the size of the pyroelectric sensitive element is reduced to a certain extent, the readout circuit becomes unable to read the pyroelectric signal. Furthermore, as mentioned earlier, the use of a chopper reduces the exposure time of the detector's sensitive element, leading to a decrease in responsivity, which also imposes constraints on reducing the size of the sensitive element to a certain extent<sup>[112, 114]</sup>.

### 3.2.3 Difficulty in integrating with ROIC

The earliest pyroelectric focal plane array devices were developed using BST ceramic materials with a hybrid structure<sup>[87]</sup>. Considering the need to improve sensitivity and reliability, the development of monolithic integrated devices is an inevitable choice. Naturally the problem of pyroelectric detection structures integrating into Si-basis of micro- and nano-electronics could not be solved without the transition from the bulk to the thin film technologies. However, some pyroelectric thin film materials with excellent performance, such as  $\text{PbTiO}_3$ ,  $\text{PbZr}_x\text{Ti}_{1-x}\text{O}_3$  (PZT), and  $\text{Pb}_x\text{Sr}_{1-x}\text{TiO}_3$  (PST), require relatively high growth temperatures, which can easily damage the

silicon-based readout circuit system<sup>[115-117]</sup>. This makes the fabrication of monolithic integrated focal plane array devices extremely challenging. In the following section, we will discuss how to address these challenges and achieve technological breakthroughs.

## 4 How can the bottleneck constraining pyroelectric focal plane arrays be broken?

The HIDAD project, which stands for "high-density infrared detector array", was a key initiative led by the U. S. Defense advanced research projects agency (DARPA) from the 1980s to the early 1990s. Its primary goal was to advance the practical application of uncooled infrared focal plane array (UFPA) technology as a replacement for the bulky, expensive, and power-hungry cooled infrared systems of the time<sup>[118]</sup>. HIDAD was a large, classified contract awarded by the U. S. Department of Defense to Honeywell, Raytheon, and the R&D group then part of Texas Instruments. The Honeywell R&D team focused on  $\text{VO}_x$  microbolometer technology, while the Raytheon team, in addition to  $\text{VO}_x$  technology, also developed BST pyroelectric technology<sup>[104, 119]</sup>.

C. M. Hanson was a core participant in the HIDAD project and was therefore very familiar with uncooled focal plane array technology, especially pyroelectric technology. To overcome the inherent requirement of a mechanical chopper in pyroelectric detection and the severe drawbacks associated with it, Hanson did propose several solutions for chopper-less pyroelectric detection technology<sup>[87, 120, 121]</sup>. However, these chopperless pyroelectric detector schemes introduced spatial noise at least as problematic as that of bolometers, and they also eliminated the  $1/f$  noise suppression afforded by AC coupling<sup>[110]</sup>. Therefore, such concepts had no practical application value. In 1996, he proposed a so-called thermal reset concept to address these problems and filed a patent for it. While this promised significant improvement, and while it was demonstrated in mechanical test pixels, it was never attempted in any kind of operational device. Recently, C. M. Hanson has made all the documents of this patent publicly available and hopes that a research institution will put his ideas into practice. The R&D team at Symetrix has developed a pyroelectric detector with an active detection mode, exhibiting an extremely high signal-to-noise ratio and a chopper-free design<sup>[122, 123]</sup>. The Smart-Cut single-crystal thin film transfer technology enables the fabrication and transfer of ferroelectric single-crystal thin films, thereby avoiding the damage to readout circuits caused by high-temperature growth of ferroelectric thin films<sup>[124]</sup>. The continuous development of the above-mentioned technologies can address the inherent shortcomings of traditional pyroelectric detectors, thereby making the development of monolithically integrated pyroelectric focal plane array detectors possible.

### 4.1 Thermal reset: a novel approach to pyroelectric imaging

Several studies have explored the basic principles of

thermal reset operation, but it has not yet been engineered in focal plane arrays. On the basis of previous concepts, this section summarizes their common advantages and looks forward to the challenges of array integration. A conventional optomechanical chopper alternately blocks and exposes the detector to the imaged scene. The chopper is constructed and positioned to provide an edge that moves vertically past one row at a time. Fig. 7 (a) shows a typical rotary chopper with an Archimedes spiral edge to best approximate horizontal edge moving vertically. The detector array is shown partially exposed and partially obscured by the chopper, and the degree of exposure increases as the chopper rotates clockwise. The desired operation is that the chopper obscuration uniformly exposes one row at a time, but real choppers can only approximate that with a blade of practical size<sup>[112, 125, 126]</sup>. An Archimedes spiral is more uniform row-to-row, but the profile of the edge is curved, leading to a small inefficiency.

As the chopper rotates, the temperature of each pixel fluctuates periodically as shown in Fig. 7 (b). Signal is optimized when the time of obscuration is equal to the time of exposure, leaving only 50% of the total available time for collecting signal. The electrical signal is generated by clamping the output at one extreme of the thermal wave and reading the signal at the next extreme. There are therefore alternating positive and negative signals. The negative signals are inverted and can then be added to the positive signals for improved responsivity [Fig. 7 (c)]. Even if the negative signal is superimposed onto the positive signal through circuit design, the theoretically improved responsivity can only reach 68.2% of the total thermal difference.

An alternative approach proposed by Hanson is to eliminate the chopper and periodically activate each pixel electrostatically to touch the substrate, as shown in Fig. 7 (d), thereby resetting its temperature<sup>[127]</sup>. Since contact with the substrate shorts the pixel thermal isolation, the thermal time constant during contact is very short<sup>[128, 129]</sup>. That means that contact time can be very short, leaving more time for signal collection. The signal for thermal reset operation is significantly larger than with a chopper, but the advantage diminishes for longer exposure times. Both phases of the chopped signal can contribute to responsivity, although half of the readings do not contain any new scene information. In what follows we shall investigate the implications of these ideas. The amplitude of the waveform, shown in Fig. 7 (e), is substantially greater than that shown for a chopped sensor, also shown for comparison. The amplitude of the thermal reset signal is 81.1% of the total thermal difference. That amounts to an 18.9% improvement over the 68.2% signal for a chopped sensor. The responsivity improvement gained from thermal reset stems from the nonlinear rate of change in pixel temperature when the scene temperature changes<sup>[130]</sup>.

This detector with a thermal reset design not only eliminates the chopper but also significantly improves responsivity, which is beneficial for reducing the size of

the detection element. As Hanson claimed, this thermal reset design of the detector can eliminate all the objections of traditional pyroelectric detectors with a chopper<sup>[133, 134]</sup>. There are ample reasons to desire a pyroelectric solution for uncooled thermal imaging. However, as with any technology of this kind, its development will cost tens of millions of dollars and require about ten years to complete. The spectacular progress of microbolometers over the past two decades has raised the bar for competing technologies to a level that was unimaginable ten years ago. Anyone wishing to pursue competitive research and development using the technology described herein must carefully analyze its performance potential<sup>[135, 136]</sup>.

We consider that the key to realizing the thermally reset pyroelectric detector lies in the design of the mechanical thermal exchange between the sensitive detection element and the substrate. This thermal exchange design can draw inspiration from the highly efficient electrocaloric cooling design proposed by Ma et al<sup>[132]</sup>. Electrostatic actuation forces are used to achieve rapid thermal exchange of the EC stack between the heat source and heat sink. Fig. 7 (f) shows that electrostatic actuation brings the EC polymer stack into contact with the top heat-dissipating aluminum plate. During this process, heat is transferred from the EC polymer stack to the heat sink. Fig. 7 (g) shows that electrostatic actuation brings the EC polymer stack into contact with the aluminum plate serving as the heat source. During this process, heat is transferred from the heat source to the EC polymer stack. Combining these two processes enables rapid heat exchange. The EC stack could be shuttled rapidly with a response time of less than 30 ms and total energy consumption of only  $\sim 0.02 \text{ W}$ <sup>[132]</sup>.

#### 4.2 Active mode detection with enhanced pyroelectric sensitivity

Recently Colorado based Symetrix Corporation in collaboration with auto supplier giant Delphi and Argonne National Laboratory describes a comprehensive development program of FPA pyroelectric detectors that incorporate active multispectral detection and are capable of providing greatly enhanced imaging performance using very low-cost fabrication techniques<sup>[122, 137]</sup>. They have developed a principle prototype and demonstrated several excellent characteristics: 1) high signal-to-noise ratio resulted from both the enhanced pyroelectric coefficient via polarization switching and drastic noise reduction<sup>[138]</sup>; 2) chopper-less design due to the electronic switching in AC-mode<sup>[123, 138]</sup>; 3) MEMS-less structure with a novel thermal isolation scheme<sup>[123, 138]</sup>; 4) spectral optimization of responsivity using interferometric approach<sup>[123, 139]</sup>.

Conventional thin-film pyroelectric detectors often suffer from performance degradation of the ferroelectric thin film (as compared to their bulk counterparts)<sup>[140]</sup>. In 2007, the research teams of Delphi and Symetrix publicly demonstrated an alternative means with an active pyroelectric detection (APD) mode. Such active approach yields several distinct advantages over its passive counterparts, including greater effective pyroelectric coef fi

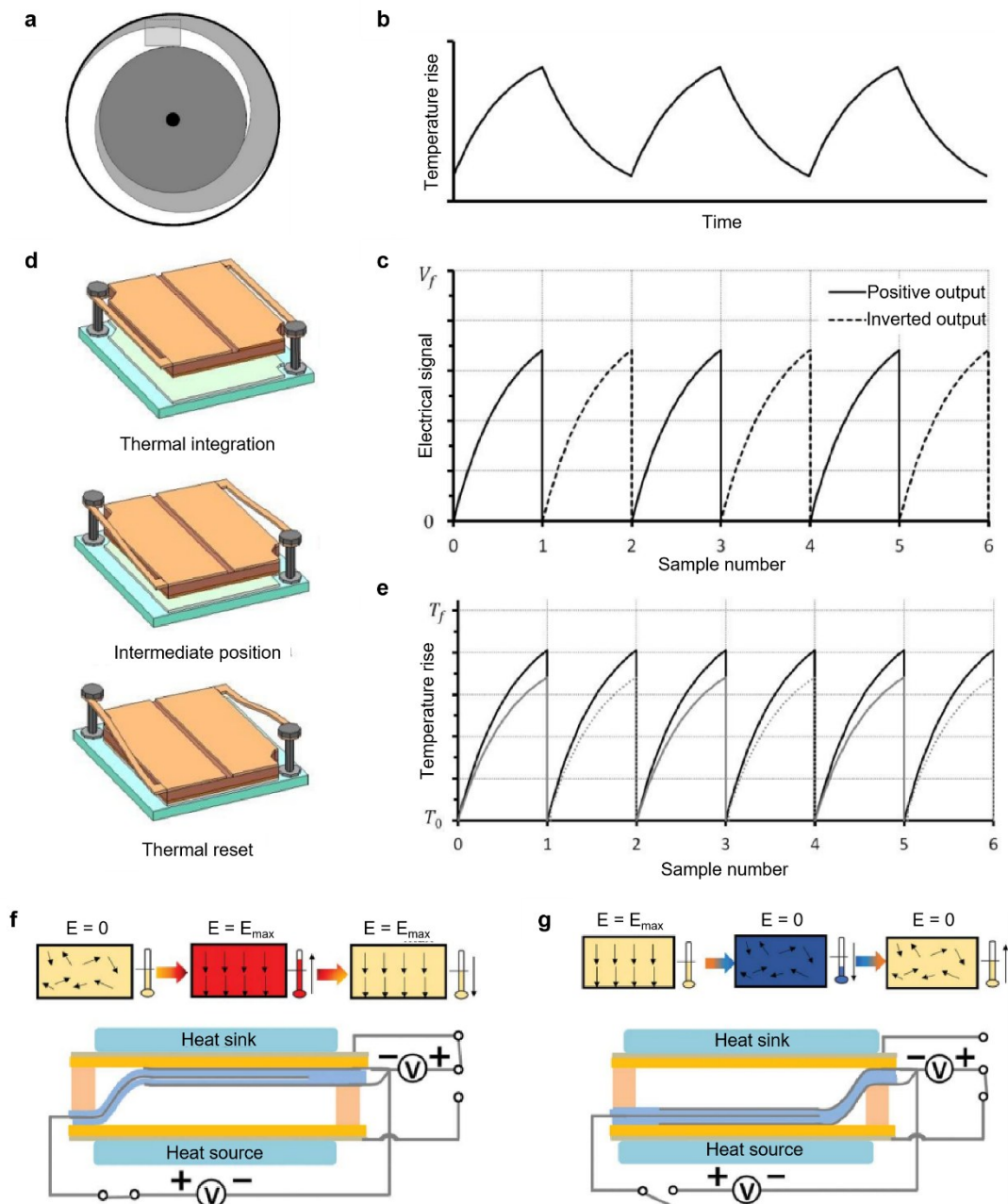


Fig. 7 A novel approach to thermal reset: (a) Schematic diagram of a rotating chopper<sup>[112]</sup>; (b) When the chopper is operating, the temperature of each pixel fluctuates periodically<sup>[131]</sup>; (c) The electrical signal is generated by clamping the output at one extreme of the thermal wave and reading the signal at the next extreme, which produces an alternating positive-negative signal<sup>[131]</sup>; (d) Periodically activating each pixel by electrostatic means to contact the substrate, thereby resetting the temperature; (e) Comparison of the signal from thermal resetting and the signal from the chopper<sup>[131]</sup>; (f) Electrostatic actuation brings the electrocaloric (EC) polymer stack into contact with the top heat-dissipating aluminum plate. During this process, heat is transferred from the EC polymer stack to the heat sink<sup>[132]</sup>; (g) Electrostatic actuation brings the EC polymer stack into contact with the aluminum plate serving as the heat source. During this process, heat is transferred from the heat source to the EC polymer stack<sup>[132]</sup>.

图7 一种新的热复位方法:(a)旋转式斩波器的示意图[112];(b)当斩波器运行时,每个像素的温度会周期性波动[131];(c)通过控制输出在热波的一个极值并读取下一个极值的信号来产生电信号,从而产生交替的正负信号[131];(d)通过静电方式周期性激活每个像素以接触基板,从而复位温度;(e)热复位信号与斩波器信号的比较[131];(f)静电驱动使电热制冷聚合物堆与顶部的散热铝板接触。在此过程中,热量从电热制冷聚合物堆传递到散热器[132];(g)静电驱动使电热制冷聚合物堆与作为热源的铝板接触。在此过程中,热量从热源传递到电热制冷聚合物堆[132]。

cient and improved signal to noise ratio.

APD departs substantially from conventional modes of operation in that the polarization state of the material is interrogated by changing it, analogous to what has been

traditionally done in ferroelectric random access memory (FeRAM) nonvolatile memory devices<sup>[122]</sup>. The individual ferroelectric capacitor elements comprising a pyroelectric FPA are driven by an external potential to switch be-

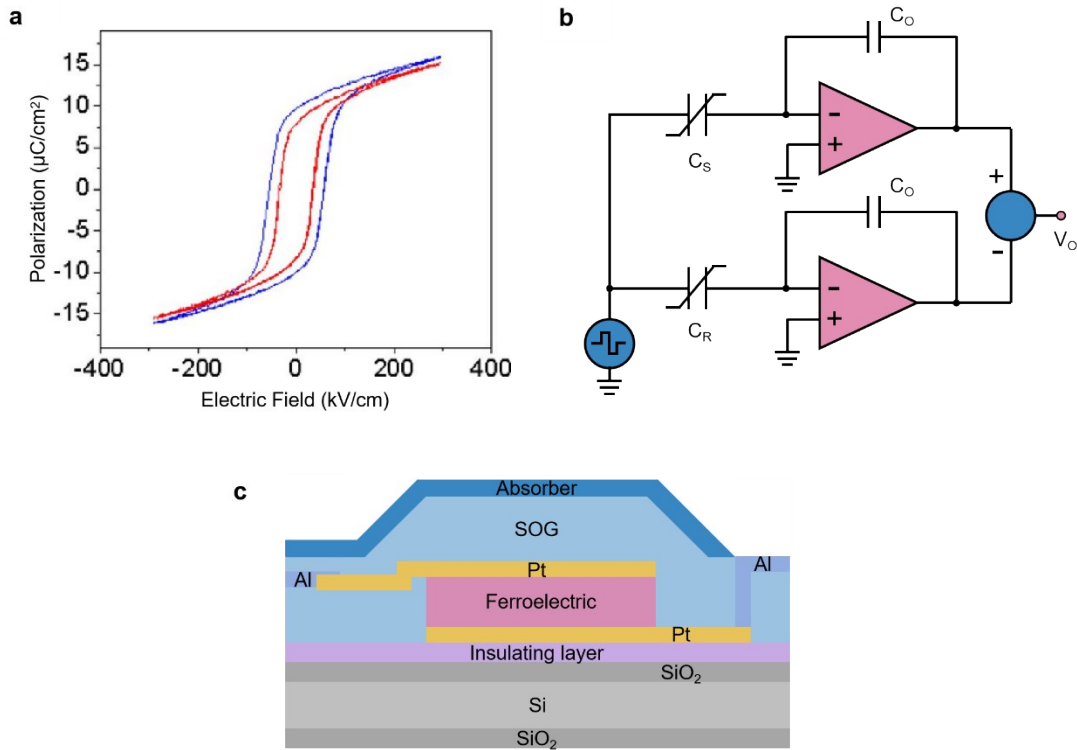


Fig. 8 Active mode detection with enhanced pyroelectric sensitivity: (a) Comparison of hysteresis loops of a typical ferroelectric thin film at room temperature and 75°C<sup>[122]</sup>; (b) The output signal of each pixel is similar to that of a differential circuit<sup>[122]</sup>; (c) The ferroelectric capacitor is isolated from the substrate by a novel nanocomposite material.

图8 具有增强型热释电灵敏度的主动检测模式:(a)室温和75°C下典型铁电薄膜的电滞回线对比图<sup>[122]</sup>; (b)每个像素的输出信号与差分电路的输出信号相似<sup>[122]</sup>; (c)铁电电容器通过一种新型纳米复合材料与基底隔离。

tween their positive and negative polarization states at voltage levels sufficiently large to achieve significant polarization switching currents. Fig. 8 (a) compares the hysteresis responses of a typical ferroelectric thin film capacitive test structure held at room temperature and then 75 °C higher<sup>[122]</sup>. The device was excited with a +5 V peak triangular wave at 10 kHz in a Sawyer-Tower configuration. Note that the difference in polarization between the two curves is quite pronounced. For IR FPA imaging devices, however, the difference in  $P_s$  (due to scene temperature variations at the pixel level,  $\Delta T_p$ ) would be substantially smaller than that shown in Fig. 8 (a). Each time the polarization switches between its two extremes, a charge is supplied from the external power source. Summing the switched charge for each half-cycle gives the total charge accumulated over  $N$  cycles. The detector signal can be improved by comparing  $Q$  scene to the output of a reference element,  $Q$  reference, which has a similar area but is not exposed to radiation. The output signal per pixel is the charge difference between the scene element and the reference one, and this idea can be implemented using a circuit analogous to a differential configuration [Fig. 8 (b)]<sup>[122]</sup>. Therefore, APD effectively multiplies up the pyroelectric coefficient by twice the number of switching cycles. Note, however, that hysteretic switching results in heat dissipation due to internal losses that stem from the reorientation of the ferroelectric dipoles during cycling. In addition, piezoelectric effects

and their related loss must also be accounted for. In their study, a strontium bismuth tantalate [ $\text{SrBi}_2\text{Ta}_2\text{O}_9$  (SBT)] thin film is used as the ferroelectric and pyroelectric layer, and the switching losses have been measured and found to be exceedingly small. Notice that the noise diminishes with  $N$  as  $1/N^{1/2}$  as one would expect for random, Gaussian, white noise, and it is expected the temperature noise to decrease to the fundamental limit of pyroelectric detectors with increased  $N$ . A  $20\mu\text{m} \times 20\mu\text{m}$  pyroelectric pixel developed and tested at Symetrix provided an NETD of 23mK, which approaches to that of the current microbolometers in small-pixel configurations.

Another notable feature of the APD design is that the sensing mechanism eliminates the need for a costly, unreliable, and vibration-producing mechanical radiation chopper that is found in the traditional pyroelectric IR systems<sup>[141]</sup>. The APD pyroelectric sensor under development by Symetrix does not rely on high-cost MEMS-based methods for thermal isolation<sup>[123]</sup>. Therefore, reliability can be significantly improved and costs reduced. As shown in Fig. 8 (c), the ferroelectric capacitors are isolated from the substrate via a novel nanolaminate of metal/oxide layers. Incorporation of nanoparticles with the oxide layers provides an oxide-metallic thermal barrier that inhibits heat transport via scattering of phonons. Ti, Nb or Ta layers are grown followed by appropriate annealing to induce the growth of  $\text{TiO}_x$ ,  $\text{NbO}_x$ ,  $\text{TaO}_x$  nanoparticles. Multiple formations of layered Ta/W or Ta/

$\text{Al}_2\text{O}_3$  film will result in a layer with embedded nanoparticles that can impede the phonon propagation, thus thermal transport, leading to an efficient thermal barrier, as already demonstrated by Symetrix. At present, this mode is still in the conceptual stage in the field of pyroelectric imaging, and there have been no specific reports on focal plane devices.

### 4.3 Monolithic integrated detectors via a smart cut thin-film transfer technology

As aforementioned, monolithic integrated devices will require performing a high-temperature anneal of the ferroelectric thin films, which was a serious problem in earlier attempts because of the temperature intolerance of ROICs. Although a great deal of effort has been made to lower the temperature for growing ferroelectric thin films, the annealing temperature is still too high for the readout circuit to withstand, and the performance of the ferroelectric thin film is more or less compromised. A new development should be based on a film-transfer process, an approach that was considered in earlier efforts but rejected as unnecessary. The film-transfer process would solve several processing problems, but would not be without difficulties of its own.

Almost concurrently, in 2001, Wan *et al.* and the French company SOITECH introduced the concept of utilizing the smart-cut process to transfer  $\text{LiNbO}_3$  (LN)/LT single-crystal thin films<sup>[124, 142]</sup>. Fig. 9 (a) provides a schematic representation of the smart cut process employed to produce LN single-crystal thin films. Detailed technical details of the thin-film transfer process can be found in the relevant literature. To date, smart cut tech-

nology has achieved great success in the field of LN thin films, enabling the fabrication of single-crystal LN thin films with thicknesses ranging from tens of nanometers to one micrometer<sup>[102]</sup>. Pyroelectric devices are fabricated using the single-crystal thin films obtained by this method. This technology can also be applied to the preparation of LT thin films. The smart cut technique can be used to transfer the LT thin film onto a silicon-based readout circuit substrate. For LN/LT thin films, a common preparation method is wafer bonding, which typically yields films with thicknesses on the order of micrometers. The next key challenge is how to achieve interconnection, that is, how to firmly connect the LT electrodes with the electrodes on the readout circuit. The interconnection between the pyroelectric sensing element and the readout circuit can be achieved using an anisotropic conductive polymer. An anisotropic conductive film consists of an insulating polymer matrix and conductive micro-particles. When the anisotropic conductive film is not subjected to heat or pressure, the conductive particles dispersed in the insulating polymer remain separated from one another, and the entire film is in an insulating state. When the anisotropic conductive film is softened by heat and locally compressed vertically, the film is compressed in the thickness direction, causing the metallic or organic conductive particles dispersed in the polymer to connect along the thickness direction, thereby achieving vertical conductivity<sup>[143]</sup>.

Both the thermal reset and active detection mode designs avoid the use of a chopper, thereby effectively improving the detector's responsivity and facilitating a re-

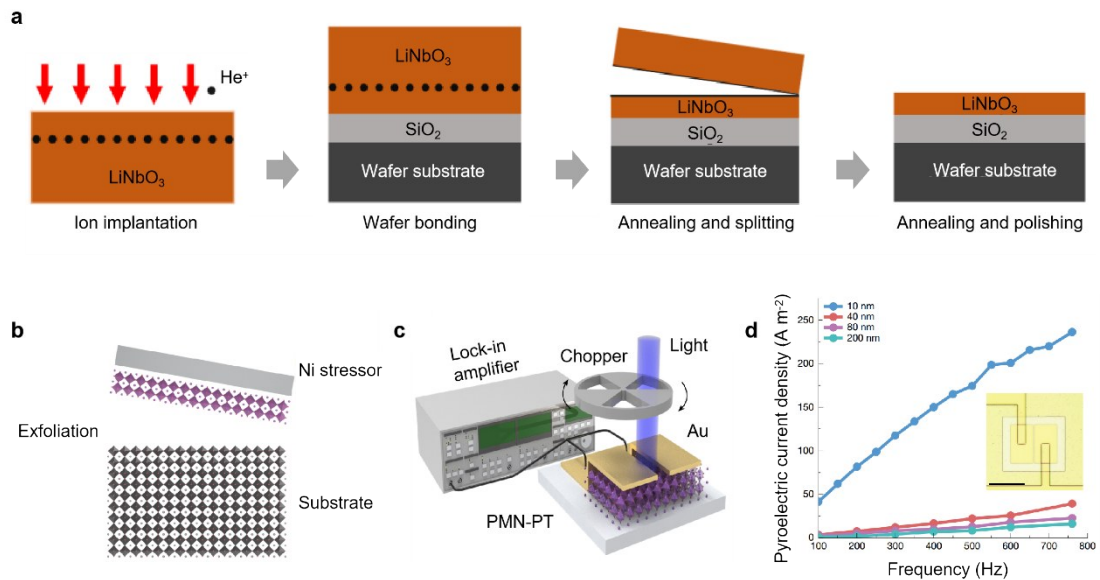


Fig. 9 Atomic lift-off of epitaxial membranes for Pyroelectric detectors: (a) Schematic diagram of the cutting process used to prepare  $\text{LiNbO}_3$  single-crystal thin films; (b) Schematics showing the peeling mode of spalling<sup>[102]</sup>; (c) Schematic diagram of a pyroelectric device fabricated using thin films obtained by atomic lift-off<sup>[102]</sup>; (d) Pyroelectric current density as a function of measurement frequency for  $\text{Pb}(\text{Mg}_{1/3}\text{Nb}_{2/3})\text{O}_3\text{-PbTiO}_3$  (PMN-PT) with different thicknesses. The inset is the optical microscopic image of a single pyroelectric device<sup>[102]</sup>.

图9 用于热释电探测器的外延膜的原子级剥离:(a)用于制备铌酸锂单晶薄膜的切割工艺示意图;(b)剥落模式的示意图[102];(c)使用通过原子剥离获得的薄膜所制备的热释电器件示意图[102];(d)不同厚度的铅镁铌酸氧铅材料的热释电电流密度随测量频率的变化曲线。插图为单个热释电器件的光学图像[102]。

duction in the sensing element size. Meanwhile, reducing the thickness of the ferroelectric thin film helps increase the capacitor's capacitance, which also has a positive effect on reducing the sensing element size<sup>[144, 145]</sup>. Therefore, the crystal ion slicing (CIS) method mentioned earlier is not suitable here. The physical vapor deposition (PVD) method allows flexible control over the thickness of pyroelectric thin films, but to maintain the pyroelectric performance of LN or LT, the adjustable thickness range is actually limited. In contrast, PZT thin films maintain excellent pyroelectric properties over a wide thickness range. Thus, when using PVD to prepare PZT thin films, the thickness can be adjusted from nanometers to micrometers while still maintaining a high pyroelectric coefficient. The chemical vapor deposition (CVD) is also a common method for preparing pyroelectric thin films, but the pyroelectric coefficient of the resulting films fluctuates significantly. The sol-gel method can produce thinner pyroelectric films than the previous methods, which is very helpful for reducing device dimensions. If device miniaturization is not required, then PZT thick films are the best choice. Their performance approaches that of bulk materials, showing unique advantages in fields such as uncooled infrared focal plane arrays and high-power laser detection. Currently, PZT thick films are mainly prepared by screen printing, and their pyroelectric coefficient can reach  $380 \mu\text{C m}^{-2} \text{K}^{-1}$  (Table 2).

Very recently Zhang et al introduce a technique that achieves atomic precision lift-off of ultrathin membranes without artificial release layers to facilitate the high-throughput production of scalable, ultrathin, freestanding ferroelectric perovskite systems, as shown in Fig. 9 (b)<sup>[102]</sup>. In their report, a record-high pyroelectric coefficient was achieved using the thickness effect of freestanding membranes [Fig. 9 (c)]. And pyroelectric device arrays with a 100% yield have been fabricated, which promise cooling-free FIR detectors exceeding the performance of conventional HgCdTe-based devices [Fig. 9

(d)]. Nevertheless, when such an ultrathin membrane with a high pyroelectric coefficient is employed in a pyroelectric FPA, it enables a substantial reduction in the size of the individual sensing elements. With the advancement of technology, flexible pyroelectric materials have found widespread applications in many fields, among which PVDF is the most prominent. At present, PVDF is mainly prepared by spin-coating, which allows flexible control of film thickness and pyroelectric coefficient by varying the number of spin-coated layers. In contrast, the Langmuir-Blodgett (LB) method can directly obtain a high content of the  $\beta$  phase without post-treatment, yielding films with superior performance; however, this method is difficult to scale up for large-area films and suffers from low throughput (Shown as table 2). Nowadays, thanks to innovative detector structure designs and advances in thin-film deposition techniques, the inherent challenges facing pyroelectric focal plane array technology are being gradually resolved, opening up broad prospects for its development.

## 5 Emerging trends and future directions

### 5.1 Integration with artificial intelligence and machine learning

The integration of single-element and multi-element pyroelectric detectors with artificial intelligence (AI) and machine learning (ML) algorithms will bring greater potential and more applications to traditional pyroelectric detector applications, enabling higher sensitivity and faster response in more complex application environments. It focuses on the advantages and challenges of triglycine sulfate (TGS) in thermal imaging, gas sensing, and security systems, and compares the performance of various long wavelength infrared pyroelectric materials, such as TGS, PZT, PVDF, and others<sup>[166]</sup>. Future research in this area is likely to focus on developing more sophisticated AI models tailored to the unique characteristics of pyroelectric signals, enabling advanced features such as automatic scene interpretation and anomaly de-

**Table 2 Preparation methods of pyroelectric thin films and their corresponding thickness and pyroelectric coefficient.**

图2 热释电薄膜的制备方法和相应的厚度与热释电系数

Pyroelectric thin film	Method	Thickness	$p$ ( $\mu\text{C m}^{-2} \text{K}^{-1}$ )	References
PZT	screen printing	10–100 $\mu\text{m}$	90–380	[146–148]
	PVD	0.8–2 $\mu\text{m}$	300	[149, 150]
	CVD	2 $\mu\text{m}$	50–300	[151, 152]
	sol-gel method	500 nm	290	[153]
LiNbO <sub>3</sub>	CIS	9–10 $\mu\text{m}$	50	[154]
	PVD	300–500 nm	71	[155]
	CVD	120–500 nm	—	[156]
	sol-gel method	970–1400 nm	27–45	[157, 158]
LiTaO <sub>3</sub>	CIS	0.1–1 $\mu\text{m}$	200	[159]
	PVD	400 nm	40–60	[160, 161]
	sol-gel method	500 nm	400	[162, 163]
PVDF	LB	90 nm	26.7	[164]
	spin-coated	1.7 $\mu\text{m}$	20	[100, 165]

tection in various applications.

Although pyroelectric detectors have encountered many difficulties and challenges in infrared imaging applications, research and development of related technologies have not ceased. In the industrial sector, Tanaka *et al.* demonstrated a high-speed thermal imaging system for production line monitoring, utilizing a linear array of 1024 TGS detectors<sup>[167]</sup>. The system operated at frame rates up to 1 kHz, enabling real-time detection of thermal defects in products moving at speeds of 10 m/s.

## 5.2 Ultrafast response

A pivotal trend in the advancement of pyroelectric infrared detectors is the transition from conventional thermal detection limits to achieving ultrafast response times, effectively overcoming the inherent speed constraints imposed by the thermal diffusion process. Traditional pyroelectric detectors, which rely on a relatively thick absorption layer and the subsequent diffusion of heat to the pyroelectric element, are fundamentally limited to response times on the order of microseconds to milliseconds. This bottleneck has historically precluded their application in scenarios requiring high-speed signal acquisition, such as real-time spectroscopy and high-frequency event detection. Recent breakthroughs, however, have demonstrated a paradigm shift by integrating nanophotonic structures, most notably plasmonic metasurfaces, into the detector architecture<sup>[168]</sup>. The advancement of two key technologies, namely the fabrication of ultrathin pyroelectric functional layers and the application of metallic metasurfaces, ensures ultra-high response speed in future pyroelectric detectors. Researchers at the Fraunhofer Institute and Massachusetts Institute of Technology have demonstrated that atomic-layer deposition (ALD) and atomic lift-off techniques can produce ultra-thin pyroelectric films with record-breaking performance. For example, single-crystal PMN-PT films just 10 nanometers thick exhibit a pyroelectric coefficient as high as  $1.76 \times 10^{-2} \text{ C}/(\text{m}^2 \cdot \text{K})$ , two orders of magnitude higher than conventional thin films<sup>[102]</sup>. Meanwhile, ALD-grown La: HfO<sub>2</sub> films are fully CMOS-compatible, offering a practical path to monolithic integration with silicon readout circuits<sup>[169, 170]</sup>. This atomic-level engineering of materials enables wafer-scale uniformity and the ability to tailor pyroelectric properties with unprecedented precision. Future imagers will be built on a foundation of “ideal” pyroelectric materials that combine ultra-high sensitivity, low dielectric loss, and high Curie temperature, essential characteristics for high-performance infrared detection without cryogenic cooling. In addition, Duke University’s recent breakthrough proves this is not an inherent limitation of the pyroelectric effect itself, but rather a constraint of conventional device architectures<sup>[171]</sup>. By integrating a plasmonic metasurface, composed of silver nanocube arrays on an ultra-thin gold film, the Duke team achieved a pyroelectric detector with a bandwidth of 2.8 GHz, corresponding to a response time of just 125 picoseconds. This is thousands of times faster than traditional pyroelectric devices. The metasurface confines incident light energy within a sub-

wavelength volume through plasmonic effects, allowing the use of an extremely thin pyroelectric layer with minimal thermal mass. This elegant design bypasses the classical trade-off between optical absorption and thermal response time<sup>[171]</sup>. As a result, high-speed, uncooled infrared imaging becomes feasible, enabling applications such as high-frame-rate thermal video, microsecond-scale transient event analysis, and even thermal light detection and ranging (LiDAR), applications traditionally dominated by expensive, cryogenically cooled photon detectors.

Therefore, it is reasonable to infer that employing the atomic lift-off (ALO) technique for growing pyroelectric functional thin films, together with integrating metallic metasurfaces into the detector architecture, can yield pyroelectric infrared detectors possessing ultra-high sensitivity and ultra-fast response, rivaling the performance of conventional cooled infrared photodetectors.

## 5.3 The future directions of pyroelectric detectors in infrared imaging

The convergence of several breakthrough technologies, including atomic-layer-grown pyroelectric thin films, plasmonic metasurface integration onto pyroelectric detection elements, thermal reset mechanisms, and active mode detection, is poised to fundamentally transform pyroelectric infrared imaging<sup>[102]</sup>. No longer constrained to cost-sensitive, low-performance applications, the pyroelectric detector is evolving into a high-speed, intelligent, and versatile imaging platform. These advances directly address the fundamental limitations of conventional pyroelectric detectors, namely poor sensitivity, slow temporal response, inability to image static scenes, and dependence on mechanical choppers. Collectively, they herald a new era for uncooled infrared technology.

Ultra-high sensitivity combined with GHz speed becomes possible when atomic-layer-grown films provide the material foundation for Duke’s metasurface architecture. The resulting detector can capture subtle temperature differences at microsecond timescales, enabling applications such as early-stage inflammation detection in medical diagnostics or microsecond-resolution combustion analysis in industrial research<sup>[168]</sup>. Chopper-less, all-solid-state operation is achieved through Symetrix’s active mode detection (AMD) technology<sup>[138]</sup>. Without moving parts, the imager becomes compact, rugged, and power-efficient, ideal for deployment in drones, wearable devices, and space missions where reliability and low mass are paramount. The elimination of the mechanical chopper also removes a major cost driver, making high-performance thermal imaging more accessible. True static scene imaging finally becomes practical through the combination of thermal reset and AMD<sup>[139]</sup>. The classical “dynamic-only” limitation of pyroelectric detectors is overcome, enabling staring-mode operation for surveillance, medical thermography, and industrial inspection without mechanical scanning or external modulation. On-chip multi-spectral and hyperspectral imaging emerges naturally from the metasurface approach<sup>[171]</sup>. Duke’s structure is inherently wavelength-selective; by integrat-

ing pixels with different metasurface geometries on the same chip, a single focal plane array can simultaneously capture infrared “fingerprints” at multiple wavelengths. This enables material identification, gas detection, and precision agriculture monitoring without external filter wheels or tunable sources. Adaptive, intelligent vision becomes the defining feature of future pyroelectric imagers. AMD’s dynamic partitioning capability allows the sensor to mimic biological retinas through a foveated architecture. The imager can allocate high resolution, high sensitivity, and high frame rates to regions of interest, such as a pedestrian in a night-driving scene, while monitoring the background at low power and low data rate. When combined with on-chip AI accelerators, the sensor becomes an intelligent perception engine rather than a passive image transmitter<sup>[172]</sup>.

#### 5.4 Difficulties and challenges for future pyroelectric FPA technology

While recent breakthroughs have dramatically advanced pyroelectric FPA technology, several significant challenges remain on the path to widespread adoption and high-performance applications. These challenges span materials science, device physics, manufacturing, and system integration (Table 3).

##### 5.4.1 Materials and fabrication challenges

Although atomic lift-off techniques have demonstrated record pyroelectric coefficients of  $1.76 \times 10^{-2} \text{ C} \cdot \text{m}^{-2} \cdot \text{K}^{-1}$  in ultra-thin single-crystal PMN-PT membranes, transitioning these laboratory-scale demonstrations to wafer-level, high-throughput manufacturing remains formidable<sup>[102]</sup>. The atomic lift-off process relies on precise control of epitaxial growth and interface chemistry, specifically the weakening of chemical bonds using lead elements at the interface. Reproducing this with high yield across 200 mm or 300 mm wafers presents substantial engineering hurdles.

Uniformity across large arrays

For large FPA containing over 1000,000 individual sensitive elements, pixel-to-pixel uniformity in pyroelectric coefficient, dielectric constant, and thermal isolation is essential. Any variation manifests as fixed pattern noise (FPN) that degrades image quality. Achieving sub-percent uniformity across large-area arrays using emerging materials like ALD-grown La:HfO<sub>2</sub> or transferred single-crystal membranes remains an unsolved challenge<sup>[173, 174]</sup>. Even the 10 nm thickness variations can significantly alter device performance.

The RC time constant bottleneck

The Duke University metasurface-enhanced detector achieved 2.8 GHz bandwidth, corresponding to a 125 picosecond rise time. However, the same study revealed that even their smallest devices are limited by resistance-capacitance (RC) time constants rather than thermal diffusion. As pixel dimensions shrink to increase spatial resolution, the capacitance decreases, but readout parasitics become increasingly dominant<sup>[175]</sup>. Finite element simulations suggest thermal response times as fast as 30 ps may be achievable, but realizing this will require revolutionary advances in readout circuit design and pixel-

level impedance matching.

The sensitivity-speed trade-off

High-speed operation inherently competes with sensitivity. The signal-to-noise ratio of a pyroelectric detector scales with the temperature change rate—faster signals produce larger currents. However, at gigahertz frequencies, the integration time becomes extremely short (nanoseconds or less), collecting far fewer photons per pixel compared to conventional microsecond-scale integration. Achieving NETD competitive with microbolometers (typically <50 mK) at GHz frame rates requires either dramatically higher pyroelectric coefficients or novel signal integration schemes<sup>[176]</sup>.

Thermal reset and static scene imaging

CM Hanson’s thermal reset technique addresses the classical limitation of pyroelectric detectors, specifically their inability to image static scenes without modulation<sup>[177]</sup>. However, implementing thermal reset across an entire FPA while maintaining uniform reset timing and avoiding image artifacts introduces significant ROIC complexity<sup>[178]</sup>. The reset mechanism must be carefully synchronized with the frame readout, and any timing mismatch creates spatial noise patterns. Moreover, the reset process itself injects charge noise that must be managed<sup>[110]</sup>.

##### 5.4.2 Manufacturing and yield challenges

Wafer-level testing and calibration

Pyroelectric FPAs require extensive non-uniformity correction (NUC) calibration to compensate for pixel-to-pixel variations. Each device must be characterized across multiple temperature setpoints, with gain and offset correction matrices calculated and stored in on-chip memory. For high-volume manufacturing, this calibration process must be automated and completed within production takt times. The thermal and electrical precision required, often millikelvin temperature stability and sub-picoamp current measurements, pushes the limits of automated test equipment.

Packaging and thermal management

Pyroelectric detectors respond to any temperature change, including self-heating from the ROIC and ambient temperature fluctuations. The package must provide: (1) a vacuum or low-thermal-conductivity environment to thermally isolate each pixel, (2) an infrared-transparent window (typically germanium or chalcogenide glass) that maintains optical quality across the operating temperature range, and (3) efficient heat sinking for the ROIC without creating thermal gradients across the FPA. Meeting all three requirements while maintaining low cost and high reliability is nontrivial<sup>[179]</sup>.

##### 5.4.3 System integration challenges

Chopperless operation trade-offs

AMD eliminates the mechanical chopper by electrically modulating the pyroelectric material’s polarization state<sup>[138]</sup>. While this reduces size, weight, and power (SWaP), it introduces new constraints. The modulation scheme must be carefully designed to avoid aliasing with the scene’s temporal dynamics. Furthermore, the electrical modulation consumes power and can generate heat

表 3 热释电探测器所面临的挑战及相应的策略。

Table 3 Challenges and corresponding strategies of pyroelectric detectors.

Challenges	Questions	Strategies
Materials and Fabrication Challenges	<ul style="list-style-type: none"> <li>◆ Uniformity Across Large Arrays</li> <li>◆ The RC Time Constant Bottleneck</li> <li>◆ The Sensitivity-Speed Trade-off</li> <li>◆ Thermal Reset and Static Scene Imaging</li> </ul>	<ul style="list-style-type: none"> <li>◆ Precision thin-film process</li> <li>◆ Reduce circuit impedance</li> <li>◆ Minimize component size</li> <li>◆ Novel materials and novel mechanisms</li> <li>◆ Active optical modulation or electronic reset</li> </ul>
Manufacturing and Yield Challenges	<ul style="list-style-type: none"> <li>◆ Wafer-Level Testing and Calibration</li> <li>◆ Packaging and Thermal Management</li> </ul>	<ul style="list-style-type: none"> <li>◆ Develop on-chip/self-calibration structures</li> <li>◆ Enhance process testability</li> <li>◆ High-quality vacuum packaging</li> <li>◆ Low-thermal-resistance heat dissipation</li> </ul>
System Integration Challenges	<ul style="list-style-type: none"> <li>◆ Chopperless Operation Trade-offs</li> <li>◆ Multispectral Capability and Complexity</li> <li>◆ Cost Competitiveness</li> <li>◆ Thermal Diffusion Limits</li> </ul>	<ul style="list-style-type: none"> <li>◆ Active modulation and intelligent algorithms</li> <li>◆ Multi-channel discrete hybrid integration</li> <li>◆ Preference for low-cost materials</li> <li>◆ Systematic thermal management design</li> </ul>

that affects detector performance. For low-power applications (e. g. , drones, wearables<sup>[180]</sup>), this trade-off between eliminating the chopper and the power cost of AMD must be carefully evaluated<sup>[139]</sup>.

Multispectral capability vs. complexity

Metasurface-based wavelength selectivity offers the tantalizing prospect of on-chip multispectral imaging. However, integrating multiple metasurface geometries across a single FPA, each optimized for a different spectral band, requires complex, multi-step nanofabrication processes. The metasurface structures (silver nanocubes spaced 10 nm above a gold film) are extremely sensitive to process variations<sup>[181]</sup>. Any deviation in nanocube size, spacing, or alignment shifts the resonant wavelength, creating spectral crosstalk between pixels intended for different bands.

Cost competitiveness

Despite the potential performance advantages, pyroelectric FPAs must compete with mature, high-volume microbolometer technology. Uncooled microbolometers, while slower, benefit from decades of manufacturing optimization, established supply chains, and proven reliability. Pyroelectric detectors will need to demonstrate clear performance advantages in specific applications (e. g. , high-speed imaging, multi-spectral detection) to justify the development costs and overcome the incumbent technology's inertia.

Thermal diffusion limits

Even with metasurface-enhanced light trapping, the fundamental process of heat diffusion from the absorber through the pyroelectric layer sets a lower bound on response time<sup>[182]</sup>. The Duke team's simulations suggest thermal response times as low as 30 ps may be achievable, but this approaches the regime where phonon transport becomes ballistic rather than diffusive<sup>[175]</sup>. At

these time scales, traditional continuum thermal models break down, and quantum thermal transport effects may impose new limits<sup>[171, 183]</sup>.

The future of pyroelectric FPA technology is extraordinarily promising, with recent demonstrations proving that fundamental limitations of speed and sensitivity can be overcome through metasurface engineering, atomic-scale materials synthesis, and advanced readout architectures. However, transitioning these laboratory breakthroughs to robust, manufacturable, and cost-effective commercial products requires solving substantial challenges in materials integration, uniformity control, high-speed readout, and system-level optimization. The path forward lies in cross-disciplinary collaboration between materials scientists, circuit designers, packaging engineers, and application developers to address these challenges systematically.

## Acknowledgment

This work is supported by the National Natural Science Foundation of China (Grant Nos. 62588101, 62535018, 62404232), Department of Science and Technology of Yunnan Province (Grant No. 202402AC08 0002), China National Postdoctoral Program for Innovative Talents (Grant No. BX20240394), China Postdoctoral Science Foundation (Grant No. 2024M7634 10), Shanghai Post-doctoral Excellence Program (Grant No. 2024797).

## References

- [1] GAO X. , J. CHAI, J. WANG, et al. , Performance analysis of space GEO infrared detectors on the low temperature tail flame of aircrafts [J]. In-

- frared and Laser Engineering, 2025, 54(6): 20240539-1-20240539-13.
- [2] Guo L., P. Rao, C. Gao, et al., Adaptivedifferential event detection for space-based infrared aerial targets [J]. Remote Sensing, 2025, 17(5): 845.
- [3] YU J., S. LI, and B. XIE, Review of intelligent technology in infrared imaging tracking systems [J]. Infrared and Laser Engineering, 2025, 54(5): 20240567-1-20240567-20.
- [4] Kohli, K., Uncooled microbolometers for low-power battlefield sensors [J]. International Journal of Innovative Science and Research Technology, 2025, 10(6): 72-79.
- [5] Akhund T.M.N.U. and K. Teramoto, Privacy-concerned averaged human activeness monitoring and normal pattern recognizing with single passive infrared sensor using one-dimensional modeling [J]. Sensors International, 2025, 6: 100303.
- [6] Chen X.-Y., C.-Y. Wen, and W.A. Sethares, Multi-target PIR indoor localization and tracking system with artificial intelligence [J]. Sensors, 2022, 22(23): 9450.
- [7] He C., S. Liu, G. Zhong, et al., A non-contact fall detection method for bathroom application based on MEMS infrared sensors [J]. Micromachines, 2023, 14(1): 130.
- [8] Xiong J., Z. Zhou, H. Zhang, et al., Human motion recognition based on integrate interval grey association degree with pyroelectric sensors node [J]. IEEE Sensors Journal, 2024, 24(10): 15836-15846.
- [9] Wu C.-M., X.-Y. Chen, C.-Y. Wen, et al., Cooperative networked PIR detection system for indoor human localization [J]. Sensors, 2021, 21(18): 6180.
- [10] Kim H., N. Lamichhane, C. Kim, et al., Innovations in building diagnostics and condition monitoring: a comprehensive review of infrared thermography applications [J]. Buildings, 2023, 13(11): 2829.
- [11] Gil-Docampo M., J.O. Sanz, I.C. Guerrero, et al., UAS IR-thermograms processing and photogrammetry of thermal images for the inspection of building envelopes [J]. Applied Sciences, 2023, 13(6): 3948.
- [12] Weidong W., U. Vandana, B. John, et al., Simulation and experimental studies of an uncooled MEMS capacitive infrared detector for thermal imaging [J]. Journal of Physics: Conference Series, 2006, 34(1): 350.
- [13] Kostrzewa J., W.H. Meyer, G. Poe, et al. Addressing the challenges of thermal imaging for firefighting applications [C]. in Infrared Technology and Applications XXIX. SPIE, 2003.
- [14] Ukiwe E.K., S.A. Adeshina, and J. Tsado, Techniques of infrared thermography for condition monitoring of electrical power equipment [J]. Journal of Electrical Systems and Information Technology, 2023, 10(1): 49.
- [15] Alvarado-Robles G., F. Arellano-Espitia, M. Delgado-Prieto, et al., Non-contact intelligent fault diagnosis based on thermography, unsupervised feature modelling and deep-feature learning for assessing faults in electromechanical systems [J]. Infrared Physics & Technology, 2025, 150: 106039.
- [16] Farooq M.A., W. Shariff, D. O'callaghan, et al., On the role of thermal imaging in automotive applications: a critical review [J]. IEEE Access, 2023, 11: 25152-25173.
- [17] Wang Y., X. Fang, M. Zhu, et al. Analysis of the Application of Uncooled and Cooled Infrared Detection Technology in Intelligent Vehicles [C]. in Proceedings of the 28th International Cryogenic Engineering Conference and International Cryogenic Materials Conference 2022. Singapore, 2023.
- [18] Eugene, P., Monocular thermal imaging for pedestrian detection and ranging [J]. Optical Engineering, 2022, 62(3): 031212.
- [19] Rogalski, A., Infrared detectors: an overview [J]. Infrared Physics & Technology, 2002, 43(3): 187-210.
- [20] Kazmierkowski, M. P., Infrared and terahertz detectors [J]. IEEE Industrial Electronics Magazine, 2019, 13(3): 53-54.
- [21] Rogalski, A., Infrared detectors: status and trends [J]. Progress in Quantum Electronics, 2003, 27(2): 59-210.
- [22] Bogue, R., From bolometers to beetles: the development of thermal imaging sensors [J]. Sensor Review, 2007, 27(4): 278-281.
- [23] Deane S., N.P. Avdelidis, C. Ibarra-Castanedo, et al., Comparison of Cooled and Uncooled IR Sensors by Means of Signal-to-Noise Ratio for NDT Diagnostics of Aerospace Grade Composites [J]. Sensors, 2020, 20(12): 3381.
- [24] John David V., H. Steve, V. John, et al., Thermal detectors: mechanisms, operation, and performance [M], in Fundamentals of Infrared and Visible Detector Operation and Testing. Wiley, 2016. 85-104.
- [25] Si J., X. Xiao, Y. Zhang, et al., Pyroelectric properties and applications of lithium tantalate crystals [J]. Crystals, 2024, 14(7): 579.
- [26] Liu H., Y. Wang, K. Wang, et al., Turning a pyroelectric infrared motion sensor into a high-accuracy presence detector by using a narrow semi-transparent chopper [J]. Applied Physics Letters, 2017, 111(24): 243901.
- [27] Hossain A. and M.H. Rashid, Pyroelectric detectors and their applications [J]. IEEE Transactions on Industry Applications, 1991, 27(5): 824-829.
- [28] Volkmar N. Pyroelectric infrared detectors based on lithium tantalate: state of art and prospects [C]. in Detectors and Associated Signal Processing. SPIE, 2004.
- [29] Whatmore R.W. and S.J. Ward, Pyroelectric infrared detectors and materials—A critical perspective [J]. Journal of Applied Physics, 2023, 133(8): 080902.
- [30] Minin O.V., J. Calvo-Gallego, Y.M. Meziani, et al., Improvement of aninfrared pyroelectric detector performances in THz range using the terajet effect [J]. Applied Sciences, 2021, 11(15): 7011.
- [31] Batra A., P. Guggilla, M. Aggarwal, et al. Innovative techniques to improve performance of pyroelectric infrared detectors performance [C]. in Proceedings of the Sixth International Symposium on Dielectric Materials and Applications (ISyDMA'6). Cham, 2022.
- [32] Zhao C., Z. Liu, Q. Li, et al., Enhanced pyroelectric response of lithium niobate crystals for infrared detection applications [J]. Sensors, 2026, 26(4): 1141.
- [33] Moroz S.A., M.V. Khvyshchun, A.A. Tkachuk, et al. Investigation of features of functioning of the pyroelectric sensors in electronic security devices [C]. in 2021 IEEE 12th International Conference on Electronics and Information Technologies (ELIT). IEEE, 2021.
- [34] Jacobs E.L., S.K. Chari, C.E. Halford, et al. Pyroelectric sensors and classification algorithms for border/perimeter security [C]. in Electro-Optical and Infrared Systems: Technology and Applications VI. SPIE, 2009.
- [35] Zamshed Iqbal C., I. Masudul Haider, A. Muhammad Moinul, et al. Design and implementation of Pyroelectric Infrared sensor based security system using microcontroller [C]. in IEEE Technology Students' Symposium. IEEE, 2011.
- [36] Shankar and Mohan, Human-tracking systems using pyroelectric infrared detectors [J]. Optical Engineering, 2006, 45(10): 106401.
- [37] Movchikova A., A. Günther, N. Neumann, et al., Application of PIMNT single crystals for long-range and wide FOV IR

- flame detection [J]. *tm - Technisches Messen*, 2014, 81(3): 120-126.
- [38] Xavier K.L.B.L. and V.K. Nanayakkara, Development of an early fire detection technique using a passive infrared sensor and deep neural networks [J]. *Fire Technology*, 2022, 58(6): 3529-3552.
- [39] Toreyin B.U., E.B. Soyer, O. Urfalioglu, et al. Flame detection using PIR sensors [C]. in **2008 IEEE 16th Signal Processing, Communication and Applications Conference**. IEEE, 2008.
- [40] Erden F., B.U. Töreyn, E.B. Soyer, et al. Wavelet based flame detection using differential PIR sensors [C]. in **2012 20th Signal Processing and Communications Applications Conference (SIU)**. IEEE, 2012.
- [41] Tan X., H. Zhang, J. Li, et al., Non-dispersive infrared multi-gas sensing via nanoantenna integrated narrowband detectors [J]. *Nature Communications*, 2020, 11(1): 5245.
- [42] Aldhafeeri T., M.-K. Tran, R. Vrolyk, et al., A review of methane gas detection sensors: recent developments and future perspectives [J]. *Inventions*, 2020, 5(3): 28.
- [43] Christofides C. and A. Mandelis, Operating characteristics and comparison of photopyroelectric and piezoelectric sensors for trace hydrogen gas detection. I. Development of a new photopyroelectric sensor [J]. *Journal of Applied Physics*, 1989, 66(9): 3975-3985.
- [44] Song F., G.-I. Li, N. Song, et al., Design and implementation of differential mid-infrared carbon monoxide detector [J]. *Optoelectronics Letters*, 2013, 9(5): 385-388.
- [45] Dong M., C. Zheng, S. Miao, et al., A mid-infrared carbon monoxide sensor system using wideband absorption spectroscopy and a single-reflection spherical optical chamber [J]. *Infrared Physics & Technology*, 2017, 85: 450-456.
- [46] Sharma A., V. Gupta, J.G. Son, et al., Linearity of fast and highly sensitive LiTaO<sub>3</sub> pyroelectric detectors in the terahertz range [J]. *IEEE Transactions on Terahertz Science and Technology*, 2024, 14(6): 823-829.
- [47] Touayar O., N. Sifi, T. Ktari, et al., Experimental evaluation of a pyroelectric detector linearity used for pulsed laser energy absolute measurement [J]. *Sensors and Actuators A: Physical*, 2005, 120(2): 482-489.
- [48] Odon, A., Processing of signal of pyroelectric sensor in laser energy meter [J]. *Measurement Science Review*, 2001, 1(1): 215-218.
- [49] Wubs J.R., U. Macherius, X. Lü, et al., Performance of a high-speed pyroelectric receiver as cryogen-free detector for terahertz absorption spectroscopy measurements [J]. *Applied Sciences*, 2024, 14(10): 3967.
- [50] Yangtao W., W. Jing, L. Gao, et al., Split ring hole metamaterial-enhanced pyroelectric detector for efficient multi-narrowband terahertz detection [J]. *Optics Express*, 2024, 32: 19779-19791.
- [51] Liang Z., Z. Liu, T. Wang, et al. High performance THz detector based on ultra-thin LiTaO<sub>3</sub> crystal [C]. in **2015 40th International Conference on Infrared, Millimeter, and Terahertz waves (IRMMW-THz)**. IEEE, 2015.
- [52] Li W., J. Wang, J. Gou, et al., Fabrication and characterization of linear terahertz detector arrays based on lithium tantalate crystal [J]. *Journal of Infrared, Millimeter, and Terahertz Waves*, 2014, 36: 42 - 48.
- [53] Wang J., J. Gou, and W. Li, Preparation of room temperature terahertz detector with lithium tantalate crystal and thin film [J]. *AIP Advances*, 2014, 4(2): 027106.
- [54] Yoon H.W., V. Khromchenko, and G.P. Eppeldauer, Improvements in the design of thermal-infrared radiation thermometers and sensors [J]. *Optics Express*, 2019, 27(10): 14246-14259.
- [55] Pohl T., P. Meindl, L. Werner, et al., Absolute calibration of the spectral responsivity of thermal detectors in the near-infrared (NIR) and mid-infrared (MIR) regions by using blackbody radiation [J]. *Journal of Sensors and Sensor Systems*, 2021, 10(1): 109-119.
- [56] Alberding B.G., J.T. Woodward, P.S. Shaw, et al., Pyroelectric detector-based method for low uncertainty spectral irradiance and radiance responsivity calibrations in the infrared using tunable lasers [J]. *Applied Optics*, 2022, 61(11): 2957-2966.
- [57] Podobedov V., G. Eppeldauer, L. Hanssen, et al. Calibration of spectral responsivity of IR detectors in the range from 0.6  $\mu\text{m}$  to 24  $\mu\text{m}$  [C]. in **Infrared Technology and Applications XLII**. SPIE, 2017.
- [58] Pohl T., P. Meindl, J. Hollandt, et al., Particularities of pyroelectric detectors in absolute measurements of chopped radiation shown for the example of a spectral responsivity calibration in the near- and mid-infrared spectral range at two primary radiometric standards [J]. *Journal of Sensors and Sensor Systems*, 2022, 11: 61-73.
- [59] Godase V., A. Mulani, A. Pawar, et al., A comprehensive review on PIR sensor-based light automation systems [J]. *International Journal of Image Processing and Pattern Recognition*, 2025, 1(1): 22-29.
- [60] Tahir M., P. Hung, R. Farrell, et al., Lightweight signal processing algorithms for human activity monitoring using dual PIR-sensor nodes [M], 2009. 150-156.
- [61] Guerrero-Rodriguez J.-M., M.-A. Cifredo-Chacon, C. Cobos Sánchez, et al., Exploiting the PIR sensor analog behavior as thermoreceptor: movement direction classification based on spiking neurons [J]. *Sensors*, 2023, 23(13): 5816.
- [62] Pijlman F. Human activity recognition in time series in PIR sensor networks with reinforcement learning for smart lighting [C]. in **2024 IEEE Sustainable Smart Lighting World Conference & Expo (LS24)**. IEEE, 2024.
- [63] Shokrollahi A., J.A. Persson, R. Malekian, et al., Passiveinfrared sensor-based occupancy monitoring in smart buildings: a review of methodologies and machine learning approaches [J]. *Sensors*, 2024, 24(5): 1533.
- [64] Liu P., S.K. Nguang, and A. Partridge, Occupancy inference using pyroelectric infrared sensors through hidden markov models [J]. *IEEE Sensors Journal*, 2016, 16(4): 1062-1068.
- [65] Stogdale N., S. Hollock, N. Johnson, et al. Array-based infrared detection: an enabling technology for people counting, sensing, tracking, and intelligent detection [C]. in **Sensors, and Command, Control, Communications, and Intelligence (C3I) Technologies for Homeland Defense and Law Enforcement II**. SPIE, 2003.
- [66] Petra H., Comparison of results of visitor arrival monitoring using regression analysis, ed. S. Hana, B. David, and M. Jakub.
- [67] Staab J., E. Udas, M. Mayer, et al., Comparing established visitor monitoring approaches with triggered trail camera images and machine learning based computer vision [J]. *Journal of Outdoor Recreation and Tourism*, 2021, 35: 100387.
- [68] Hlaváčková P., H. Slováčková, D. Březina, et al., Comparison of results of visitor arrival monitoring using regression analysis [J]. *Journal of Forest Science*, 2018, 64: 303-312.
- [69] Andersen O., V. Gundersen, L.C. Wold, et al., Monitoring visitors to natural areas in wintertime: issues in counter accuracy [J]. *Journal of Sustainable Tourism*, 2014, 22(4): 550-560.
- [70] Theocharous, E., Absolute linearity measurements on a gold-black-coated deuterated L-alanine-doped triglycine sulfate pyro-

- electric detector [J]. *Applied Optics*, 2008, 47 (21) : 3731-3736.
- [71] Theocharous, E., Absolute linearity measurements on LiTaO<sub>3</sub> pyroelectric detectors [J]. *Applied Optics*, 2008, 47 (18) : 3397-3405.
- [72] Olivier G., J. Wlassow, and L. Bonnefond. A calibration method for the measurement of IR detector spectral responses using a FTIR spectrometer equipped with a DTGS reference cell [C]. in *High Energy, Optical, and Infrared Detectors for Astronomy VI*. SPIE, 2014.
- [73] Logan J.V., Z.M. Alsaad, C.M. Sturtevant, et al., Obtaining accurate spectral response measurements of a semiconductor-based photon detector with an FTIR: Properly correcting for the pyroelectric reference detector frequency response [J]. *Journal of Applied Physics*, 2025, 138(7) : 074501.
- [74] Dong Soo K., L. Tae-Ro, and Y. Gilwon, Development of an ultra-compact mid-infrared attenuated total reflectance spectrophotometer [J]. *Optical Engineering*, 2014, 53(7) : 074108.
- [75] Chen Y., Y. Wang, Z. Wang, et al., Unipolar barrier photodetectors based on van der Waals heterostructures [J]. *Nature Electronics*, 2021, 4(5) : 357-363.
- [76] Fomina P., A. Femenias, M. Hlavatsch, et al., A portable infrared attenuated total reflection spectrometer for food analysis [J]. *Applied Spectroscopy*, 2023, 77(9) : 1073-1086.
- [77] Nakamura K., T. Ishigaki, A. Kaneko, et al., Pyroelectric infrared detector for precision earth sensor [J]. *International Journal of Infrared and Millimeter Waves*, 1989, 10(8) : 907-930.
- [78] Sinyutin S.A., A.V. Yartsev, A.Y. Kisner, et al., Simulation of a pyroelectric receiver of photodetecting system for an earth orientation device [J]. *Russian Aeronautics*, 2021, 64 (2) : 344-354.
- [79] Andreas N., H. Alexander, P. Lucia Perez, et al. Pyroelectric detector for EE9 FORUM: design and characterization [C]. in *International Conference on Space Optics—ICSO 2022*. SPIE, 2023.
- [80] Hawkins M.A., M. Watwood, M. van den Heever, et al., From opportunity to continuity: A CubeSat implementation to enhance Earth's radiation budget observations from space [J]. *EGU Sphere*, 2026, 2026 : 1-34.
- [81] Grant M., P. Kory, and T. Susan. Transfer of radiometric standards between multiple low earth orbit climate observing broadband radiometers: application to CERES [C]. in *Earth Observing Systems XII*. SPIE, 2007.
- [82] Pachot C., B. Carnicero Domínguez, H. Oetjen, et al., The infrared Fourier transform spectrometer and the infrared imager instrument concepts for the FORUM mission, ESA's 9th Earth Explorer. 2020.
- [83] Hacker A., Characterization of a Pyroelectric Detector for a Spaceborne Fourier-Transform Spectrometer. 2022.
- [84] Scott B.E. and H. Terrence. High-MTF hybrid ferroelectric IR-FPA [C]. in *Infrared Detectors and Focal Plane Arrays V*. SPIE, 1998.
- [85] William A.R., F.M. Daniel, A. Finch, et al. Microbolometer uncooled infrared camera with 20-mK NETD [C]. in *Infrared Detectors and Focal Plane Arrays V*. SPIE, 1998.
- [86] Norton, P., Understanding the NE $\Delta$ T of tactical infrared focal plane arrays [J]. *Opto-Electronics Review*, 2012, 20 (3) : 275-278.
- [87] Charles M.H., R.B. Howard, A.O. Robert, et al. Uncooled thermal imaging at Texas Instruments [C]. in *Infrared Detectors: State of the Art*. SPIE, 1992.
- [88] Ravindra N., Optical and thermal detector fundamentals, microbolometer, and readout integrated circuits [M], 2022. 133-155.
- [89] Haider S., S. Majzoub, M. Alturaigi, et al., Pair-wise serial ROIC for uncooled microbolometer array [J]. *IEIE Transactions on Smart Processing and Computing*, 2015, 4 : 251-257.
- [90] Carl D.R., N.G. Erich, and A.K. Jonathan. Improved VO<sub>2</sub> microbolometers for infrared imaging: operation on the semiconducting-metallic phase transition with negative electrothermal feedback [C]. in *Infrared technology and applications XXV*. SPIE, 1999.
- [91] Goudon V., A. Aliane, L. Dussopt, et al. Fabrication and integration of cooled polarimetric bolometer arrays for sub-mm wave detection [C]. in *2024 49th International Conference on Infrared, Millimeter, and Terahertz Waves (IRMMW-THz)*. IEEE, 2024.
- [92] Wu B., Z. Zhang, B. Chen, et al., One-step rolling fabrication of VO<sub>2</sub> tubular bolometers with polarization-sensitive and omnidirectional detection [J]. *Science Advances*, 2023, 9 (42) : eadi7805.
- [93] Hack E., L. Valzania, G. Gäumann, et al., Comparison of thermal detector arrays for off-axis THz holography and real-time THz imaging [J]. *Sensors*, 2016, 16(2) : 221.
- [94] Utermöhlen F., D.B. Etter, D. Borowsky, et al. Low-cost microbolometer with nano-scaled plasmonic absorbers for far infrared thermal imaging applications [C]. in *2014 IEEE 27th International Conference on Micro Electro Mechanical Systems (MEMS)*. IEEE, 2014.
- [95] Yu L., Y. Guo, H. Zhu, et al., Low-cost microbolometer type infrared detectors [J]. *Micromachines*, 2020, 11(9) : 800.
- [96] Cooper, J., A fast response total-radiation detector [J]. *Nature*, 1962, 194(4825) : 269-271.
- [97] Noda, M., Uncooled thermal infrared sensors: recent status in microbolometers and their sensing materials [J]. *Sensor Letters*, 2005, 3 : 194-205.
- [98] Liu D., Q. Zhao, B. Wu, et al., Suspended Graphene/LiTaO<sub>3</sub> Pyro-FeFETs for high-sensitivity uncooled infrared detection [J]. *Materials Today Electronics*, 2026, 16 :
- [99] Aleksandrova M., C. Jagtap, V. Kadam, et al., An overview of microelectronic infrared pyroelectric detector [J]. *Engineered Science*, 2021, 16(7) : 82-89.
- [100] Wang X., H. Shen, Y. Chen, et al., Multimechanism synergistic photodetectors with ultrabroad spectrum response from 375 nm to 10  $\mu$ m [J]. *Advanced Science*, 2019, 6(15) : 1901050.
- [101] Peng Y., Q. Yang, and X. Wei. High-sensitivity uncooled graphene infrared detectors based on interface-enhanced pyroelectric photogating [C]. in *2025 50th International Conference on Infrared, Millimeter, and Terahertz Waves (IRMMW-THz)*. IEEE, 2025.
- [102] Zhang X., O. Ericksen, S. Lee, et al., Atomic lift-off of epitaxial membranes for cooling-free infrared detection [J]. *Nature*, 2025, 641(8061) : 98-105.
- [103] Schossig M., V. Norkus, and G. Gerlach, Dielectric and pyroelectric properties of ultrathin, monocrystalline lithium tantalate [J]. *Infrared Physics & Technology*, 2014, 63 : 35-41.
- [104] Cole B., R. Horning, B. Johnson, et al. High performance infrared detector arrays using thin film microstructures [C]. in *Proceedings of 1994 IEEE International Symposium on Applications of Ferroelectrics*. IEEE, 1994.
- [105] Chen C., C. Li, S. Min, et al., Ultrafast silicon nanomembrane microbolometer for long-wavelength infrared light detection [J]. *Nano Letters*, 2021, 21(19) : 8385-8392.
- [106] Murros A., K. Sovanto, J. Tiira, et al., Infrared bolometers based on 40-nm-Thick Nano-Thermoelectric silicon membranes [J]. *Infrared Physics & Technology*, 2025, 145 : 105720.

- [107] Syllaios A.J., T.R. Schimert, R.W. Gooch, et al., Amorphous Silicon Microbolometer Technology [J]. MRS Online Proceedings Library, 2000, 609(1): 144.
- [108] Jiang W., T. Zheng, B. Wu, et al., A versatile photodetector assisted by photovoltaic and bolometric effects [J]. *Light: Science & Applications*, 2020, 9(1): 160.
- [109] Andresen B.F., F. Niklaus, G.F. Fulop, et al. Characterization of transfer-bonded silicon bolometer arrays [C]. in *Infrared Technology and Applications XXX*. SPIE, 2004.
- [110] Charles M.H. A novel approach to pyroelectric imaging [C]. in *Infrared Technology and Applications XLV*. SPIE, 2019.
- [111] Paul G.W. Small-satellite radiation budget instrumentation [C]. in *Small Satellite Technologies and Applications II*. SPIE, 1992.
- [112] Yu-Qing H.E., J.I.N. Wei-Qi, G.A.O. Zhi-Yun, et al., Analysis of modulating chopper used in pyroelectric uncooled FPA thermal imager--chopper's exposure efficiency [J]. *Journal of Infrared and Millimeter Waves*, 2004, 23(4): 246-250.
- [113] Pham L., W. Tjhen, C. Ye, et al., Surface-micromachined pyroelectric infrared imaging array with vertically integrated signal processing circuitry [J]. *IEEE Transactions on Ultrasonics, Ferroelectrics, and Frequency Control*, 1994, 41(4): 552-555.
- [114] Weller H.J., D. Setiadi, and T.D. Binnie, Low-noise charge sensitive readout for pyroelectric sensor arrays using PVDF thin film [J]. *Sensors and Actuators A: Physical*, 2000, 85(1): 267-274.
- [115] Schatz A., D. Pantel, and T. Hanemann, Towards low-temperature deposition of piezoelectric Pb(Zr, Ti)O<sub>3</sub>: Influence of pressure and temperature on the properties of pulsed laser deposited Pb(Zr, Ti)O<sub>3</sub> [J]. *Thin Solid Films*, 2017, 636: 680-687.
- [116] Bretos I., R. Jiménez, M. Tomczyk, et al., Active layers of high-performance lead zirconate titanate at temperatures compatible with silicon nano- and microelectronic devices [J]. *Scientific Reports*, 2016, 6(1): 20143.
- [117] Sarney W.L., J.W. Little, F.E. Livingston, et al., Low temperature growth and laser-induced phase transformation of perovskite oxide films for uncooled IR detector applications [J]. MRS Online Proceedings Library, 2009, 1199(1): 91-96.
- [118] Wood R.A. Uncooled thermal imaging with monolithic silicon focal planes [C]. in *Infrared Technology XIX*. SPIE, 1993.
- [119] Black S.H., T. Sessler, E. Gordon, et al. Uncooled detector development at Raytheon [C]. in *Infrared Technology and Applications XXXVII*. SPIE, 2011.
- [120] Charles M.H., R.B. Howard, F.B. James, et al. Advances in monolithic ferroelectric uncooled IRFPA technology [C]. in *Infrared Detectors and Focal Plane Arrays V*. SPIE, 1998.
- [121] Hanson, C.M., Hybrid pyroelectric-ferroelectric bolometer arrays [M], in *Semiconductors and Semimetals*. Elsevier, 1997. 123-174.
- [122] Mantese J.V., A.L. Micheli, N.W. Schubring, et al., Enhanced pyroelectric sensitivity using ferroelectric active mode detection [J]. *Applied Physics Letters*, 2007, 90(11): 113503.
- [123] Unglaub R.A.G., J.B. Celinska, C.R. McWilliams, et al., Characterization of second generation advanced dynamic pyroelectric focal plane array [J]. *Integrated Ferroelectrics*, 2010, 112(1): 67-78.
- [124] Aspar B., H. Moriceau, E. Jalaguier, et al., The generic nature of the Smart-Cut® process for thin film transfer [J]. *Journal of Electronic Materials*, 2001, 30(7): 834-840.
- [125] He Y., W. Jin, G. Liu, et al., Modulate chopper technique used in pyroelectric uncooled focal plane array thermal imager [J]. *Proceedings of SPIE - The International Society for Optical Engineering*, 2002, 4919: 283-288.
- [126] Eduard-Sebastian C., D. Dorin, and D. Virgil-Florin. Optical choppers: novel approaches for higher chop frequencies [C]. in *Electro-Optical and Infrared Systems: Technology and Applications XX*. SPIE, 2023.
- [127] Hanson C.M. Uncooled IR detector performance limits and barriers [C]. in *Infrared Detectors and Focal Plane Arrays VI*. SPIE, 2000.
- [128] Song, W.-B. and J.J. Talghader, Adjustable responsivity for thermal infrared detectors [J]. *Applied Physics Letters*, 2002, 81(3): 550-552.
- [129] Topaloglu N., P.M. Nieva, M. Yavuz, et al. A pixel-by-pixel thermal conductance tuning mechanism for uncooled microbolometers [C]. in *2008 1st Microsystems and Nanoelectronics Research Conference*. Ottawa, ON, Canada, 2008.
- [130] Ozan E., B. Enes, K. Seniz Esra, et al. A plasmonically enhanced pixel structure for uncooled microbolometer detectors [C]. in *Infrared Technology and Applications XXXIX*. SPIE, 2013.
- [131] Whatmore R.W., P.C. Osbond, and N.M. Shorrocks, Ferroelectric materials for thermal IR detectors [J]. *Ferroelectrics*, 1987, 76(1): 351-367.
- [132] Ma R., Z. Zhang, K. Tong, et al., Highly efficient electrocaloric cooling with electrostatic actuation [J]. *Science*, 2017, 357(6356): 1130-1134.
- [133] Beratan H.R., C.M. Hanson, and D.L. Arbuthnot. Uncooled thermal imaging with thin-film ferroelectric detectors [C]. in *2008 17th IEEE International Symposium on the Applications of Ferroelectrics*. IEEE, 2008.
- [134] Beratan H.R., C.M. Hanson, and E.G. Meissner. Low-cost uncooled ferroelectric detector [C]. in *Infrared Detectors: State of the Art II*. IEEE, 1994.
- [135] Todd M.A., P.A. Manning, P.P. Donohue, et al. Thin film ferroelectric materials for microbolometer arrays [C]. in *Infrared Technology and Applications XXVI*. SPIE, 2000.
- [136] Paul, M., Micromachined infrared detectors based on pyroelectric thin films [J]. *Reports on Progress in Physics*, 2001, 64(10): 1339.
- [137] Thompson M.P., J.R. Troxell, M.E. Murray, et al., Infrared absorber for pyroelectric detectors [J]. *Journal of Vacuum Science and Technology*, 2007, 25: 437-440.
- [138] Ricardo U., C. Jolanta, M. Christopher, et al. Active mode detection with enhanced pyroelectric sensitivity [C]. in *Infrared Technology and Applications XXXV*. SPIE, 2009.
- [139] Ricardo A.G.U., B.C. Jolanta, R.M. Christopher, et al. Advanced dynamic pyroelectric focal plane array [C]. in *Infrared Technology and Applications XXXV*. SPIE, 2010.
- [140] Butler N., J. McClelland, and S. Iwasa. Ambient Temperature Solid State Pyroelectric IR Imaging Arrays [C]. in *Infrared detectors and arrays*. SPIE, 1988.
- [141] Kovalev A., D. Wainstein, V. Vakhruhev, et al., Anomalous heat transport in nanolaminated metal/oxide multilayer coatings: plasmon and phonon excitations [J]. *Coatings*, 2020, 10(3): 260.
- [142] Scrymgeour D.A., V. Gopalan, T.E. Haynes, et al., Ultrathin slices of ferroelectric domain-patterned lithium niobate by crystal ion slicing [J]. MRS Online Proceedings Library, 2011, 681(1): 63.
- [143] LIU, N.J.W., Novel hybrid integration approach for fabrication of single crystal pyroelectric detector [J]. *Journal of Applied Optics*, 2010, 31: 313-316.
- [144] Gong J., Y. Yang, J. Luo, et al., Advancing freestanding oxide films: innovations in preparation methods and physical properties [J]. *Progress in Materials Science*, 2026, 157: 101612.

- [145] Liu Y.-C., B.-C. Chen, C.-C. Wei, et al., Thickness-dependent ferroelectricity in freestanding  $\text{Hf}_0.5\text{Zr}_0.5\text{O}_2$  membranes [J]. *ACS Applied Electronic Materials*, 2024, 6 (12): 8617-8625.
- [146] De Cicco G., B. Morten, D. Dalmonego, et al., Pyroelectricity of PZT-based thick-films [J]. *Sensors and Actuators A: Physical*, 1999, 76(1): 409-415.
- [147] Charlot B., D. Coudouel, P. Combette, et al. Pyroelectric PZT sensors screen printed on glass [C]. in 2013 Symposium on Design, Test, Integration and Packaging of MEMS/MOEMS (DTIP). IEEE, 2013.
- [148] Wu C.G., X.Y. Sun, J. Meng, et al., Fast and wide-band response infrared detector using porous PZT pyroelectric thick film [J]. *Infrared Physics & Technology*, 2014, 63: 69-73.
- [149] Fathipour M., Y. Xu, and M. Rana, Magnetron sputtered lead titanates thin films for pyroelectric applications: part 1: epitaxial growth, material characterization [J]. *Materials*, 2024, 17 (1): 221.
- [150] Wang Y., J. Yan, H. Cheng, et al., Low thermal budget lead zirconate titanate thick films integrated on Si for piezo-MEMS applications [J]. *Microelectronic Engineering*, 2020, 219: 111145.
- [151] Asakura T., K. Ishikawa, A.S. Atushi Sato, et al., Preparation and pyroelectric characteristics of  $\text{Pb}(\text{Zr}, \text{Ti})\text{O}_3$  thin films grown by metalorganic chemical vapor deposition [J]. *Japanese Journal of Applied Physics*, 1996, 35(9S): 4886.
- [152] Roeder J.F., B.A. Vaartstra, P.C. van Buskirk, et al., Liquid delivery MOCVD of ferroelectric PZT [J]. *MRS Online Proceedings Library*, 1995, 415(1): 123-128.
- [153] Iakovlev S., C.H. Solterbeck, A. Piorra, et al., Dielectric and pyroelectric properties of PZFNt/PZT bimorph thin films [J]. *Journal of Materials Science: Materials in Electronics*, 2003, 14 (3): 143-148.
- [154] Luo W., J. Luo, Y. Shuai, et al., Infrared detector based on crystal ion sliced  $\text{LiNbO}_3$  single-crystal film with BCB bonding and thermal insulating layer [J]. *Microelectronic Engineering*, 2019, 213: 1-5.
- [155] Nishida T., M. Shimizu, T. Horiuchi, et al., Electrical properties of  $\text{LiNbO}_3$  thin films by rf magnetron sputtering and bias sputtering [J]. *Japanese Journal of Applied Physics*, 1995, 34 (9S): 5113.
- [156] Bartaszyte A., V. Plausinaitiene, A. Abrutis, et al., Thickness dependent stresses and thermal expansion of epitaxial  $\text{LiNbO}_3$  thin films on C-sapphire [J]. *Materials Chemistry and Physics*, 2015, 149-150: 622-631.
- [157] Young S.-L., M.-C. Kao, and H.-Z. Chen, The properties of tantalum modified lithium niobate thin films prepared by a diol-based sol-gel process [J]. *European Physical Journal-applied Physics*, 2006, 36: 5-10.
- [158] Lo Presti F., A.L. Pellegrino, Q. Micard, et al.,  $\text{LiNbO}_3$  thin films through a Sol - Gel/Spin-Coating approach using a novel heterobimetallic lithium - niobium precursor [J]. *Nanomaterials*, 2024, 14(4): 345.
- [159] Luo J., W. Luo, K. Zhang, et al., High specific detectivity infrared detector using crystal ion slicing transferred  $\text{LiTaO}_3$  single-crystal thin films [J]. *Sensors and Actuators A: Physical*, 2019, 300: 111650.
- [160] Combette P., L. Nougaret, A. Giani, et al., RF magnetron-sputtering deposition of pyroelectric lithium tantalate thin films on ruthenium dioxide [J]. *Journal of Crystal Growth*, 2007, 304 (1): 90-96.
- [161] Nougaret L., P. Combette, and F. Pascal-Delannoy, Growth of lithium tantalate thin films by radio-frequency magnetron sputtering with lithium enriched target [J]. *Thin Solid Films*, 2009, 517(5): 1784-1789.
- [162] Kao M.C., H.Z. Chen, C.M. Wang, et al., Pyroelectric properties of sol - gel derived lithium tantalite thin films [J]. *Physica B: Condensed Matter*, 2003, 329-333: 1527-1528.
- [163] Kao M.-C., M.-S. Lee, C.-M. Wang, et al., Properties of  $\text{LiTaO}_3$  thin films derived by a Diol-Based Sol-Gel process [J]. *Japanese Journal of Applied Physics*, 2002, 41: 2982-2986.
- [164] Liu P., J. Wang, L. Tian, et al., Electric characteristics of Langmuir-Blodgett ferroelectric polymers film: high pyroelectric coefficient and low dielectric constant [J]. *Journal of Infrared and Millimeter Waves*, 2009, 28(6):
- [165] Charlot B., S. Gauthier, A. Garraud, et al., PVDF/PMMA blend pyroelectric thin films [J]. *Journal of Materials Science: Materials in Electronics*, 2011, 22(12): 1766-1771.
- [166] Triglycine sulfate (TGS) as a pyroelectric detector: advancements and applications up to 2023 [J]. *Journal of Emerging Technologies and Innovative Research*, 2024, 11(1): 523-535.
- [167] Takahara H., H. Tanaka, and M. Hashimoto, Fast thermocycling in custom microfluidic cartridge for rapid single-molecule droplet PCR [J]. *Sensors*, 2023, 23(24): 9884.
- [168] Lu Y., L. Liu, R. Gao, et al., Ultrafast near-infrared pyroelectric detector based on inhomogeneous plasmonic metasurface [J]. *Light: Science & Applications*, 2024, 13(1): 241.
- [169] Lehmkau R., D. Mutschall, A. Kaiser, et al. Fully CMOS-compatible pyroelectric infrared detector based on doped  $\text{HfO}_2$  thin film in 3D-integration [C]. in *Oxide-based Materials and Devices XIII*. SPIE, 2022.
- [170] Mart C., M. Czernohorsky, K. Kühnel, et al., Hafnium zirconium oxide thin films for CMOS compatible pyroelectric infrared sensors [J]. *Engineering Proceedings*, 2021, 6(1): 27.
- [171] Stewart J.W., J.H. Vella, W. Li, et al., Ultrafast pyroelectric photodetection with on-chip spectral filters [J]. *Nature Materials*, 2020, 19(2): 158-162.
- [172] Ma R., J. Gong, G. Liu, et al., Enabling cognitive pyroelectric infrared sensing: from reconfigurable signal conditioning to sensor mask design [J]. *IEEE Transactions on Industrial Informatics*, 2020, 16(7): 4436-4446.
- [173] Lomenzo P.D., S. Jachalke, H. Stoecker, et al., Universal Curie constant and pyroelectricity in doped ferroelectric  $\text{HfO}_2$  thin films [J]. *Nano Energy*, 2020, 74: 104733.
- [174] Jeong J., Y. Han, J. Joo, et al., Effect of La spatial uniformity on ferroelectric properties of  $\text{HfO}_2$  films deposited by atomic layer deposition method [J]. *physica status solidi (a)*, 2024, 221 (7): 2300674.
- [175] Shin E., R.E. Bangle, N.C. Wilson, et al., Metasurface-enhanced thermal photodetector operating at gigahertz frequencies [J]. *Advanced Functional Materials*, 2025, 36(22): 2420953.
- [176] Mart C., K. Kühnel, T. Kämpfe, et al., Ferroelectric and pyroelectric properties of polycrystalline La-doped  $\text{HfO}_2$  thin films [J]. *Applied Physics Letters*, 2019, 114(10): 102903.
- [177] Charles M.H., R.B. Howard, and F.B. James. Uncooled infrared imaging using thin film ferroelectrics [C]. in *Photodetectors: Materials and Devices VI*. SPIE, 2001.
- [178] Tai Ping S., C. Yuan Lung, C. Wen Yaw, et al. Novel CMOS readout techniques for uncooled pyroelectric IR FPA [C]. in *Infrared Readout Electronics IV*. SPIE, 1998.
- [179] Robinson M.K., N.M. Shorrocks, R.W. Bicknell, et al., Packaging for thermal detectors [J]. *Hybrid Circuits*, 1989, 6 (1): 25-28.
- [180] Yang R., J. Li, Y. Wang, et al., Pyroelectric polyvinylidene fluoride film prepared by a novel combining method and its application in fully flexible infrared detector [J]. *Infrared Physics &*

- Technology, 2021, 113: 103624.
- [181] Stewart J. W., G. M. Akselrod, D. R. Smith, et al., Toward multispectral imaging with colloidal metasurface pixels [J]. *Advanced Materials*, 2016, 29(6): 1602971.
- [182] Hatanaka Y., K. Kamiryo, and T. Kano, Transient thermal analysis and experiments of pyroelectric detectors [J]. *Japanese Journal of Applied Physics*, 1972, 11(12): 1788.
- [183] Su C., H. Wu, L. Dai, et al., Nonclassical heat transfer and recent progress [J]. *ASME Journal of Heat and Mass Transfer*, 2024, 147(3): 032502.

## 热释电红外探测器在红外成像领域的未来在哪里?

胡鑫锋<sup>1,2#</sup>, 吴斌民<sup>1#</sup>, 王旭东<sup>1,2,6\*</sup>, 孟祥建<sup>1,2,3,6\*</sup>, 王建禄<sup>1,4,5\*</sup>, 褚君浩<sup>1,2,4\*</sup>

(1. 中国科学院上海技术物理研究所红外科学与技术全国重点实验室, 上海 200083;

2. 中国科学院大学, 北京 100049;

3. 复旦大学义乌研究院, 浙江 义乌 322000;

4. 复旦大学未来信息技术学院光电子研究所, 上海 200433;

5. 复旦大学集成电路与微纳电子学院集成芯片与系统国家重点实验室, 上海 200433;

6. 上海市光学薄膜与光谱调制重点实验室, 上海 200083)

**摘要:**热释电探测器是一种典型的非制冷红外探测器, 由于其高灵敏度、快速响应速度、低功耗和宽光谱响应, 广泛应用于火焰和火灾报警、运动目标传感、气体探测、温度测量甚至太赫兹探测等领域。除了常规应用外, 热释电探测器在几个专业场景中提供了不可替代的优势, 包括激光参数测量、高精度光谱仪、红外探测器的光谱响应校准, 以及红外地球传感器和地球辐射收支测量等空间科学应用。然而, 在引人注目的红外成像领域, 热释电探测器确实失去了与测辐射热计的竞争, 测辐射热计是另一种重要的非制冷红外探测器。该综述总结了传统热释电探测器在成像应用中面临的固有技术挑战, 包括与读出电路集成的困难、对斩波器的要求以及像素尺寸小型化的局限性。本文提出了两种技术解决方案以解决传统热释电探测器在红外成像中的困难: 热复位模式和主动检测模式。通过技术发展和迭代, 热释电焦平面阵列器件有望实现更高的灵敏度和更低的成本, 在红外成像技术的应用领域占据一席之地。

**关键词:**热释电探测器; 非制冷红外成像; 测辐射热计; 焦平面阵列; 热复位模式